Operational experience with miscanthus feedstock at the bioliq® fast pyrolysis plant

Nicole Weih*, Andreas Niebel, Cornelius Pfitzer, Axel Funke, George Kofi Parku, Nicolaus Dahmen

Institute of Catalysis Research and Technology (IKFT), Karlsruhe Institute of Technology, Hermann-von-Helmholtz-Platz 1, 76344 Eggenstein-Leopoldshafen, Germany

*corresponding author: nicole.weih@kit.edu

ABSTRACT

Fast pyrolysis is a thermochemical process for direct liquefaction of lignocellulosic biomass that offers flexibility in terms of feedstock variability since all biomass macromolecules are converted. In contrast to this expectation, it is also obvious that there are limits to feedstock flexibility once a fast pyrolysis plant has been built. This relates to the simple fact that any pretreatment is to a certain extent specific for one type of biomass, but also to the observation that liquid yield can vary widely depending on the feed. Different bio-oil yields directly affect heat management and volume flows in an installation. Laboratory equipment has very limited suitability to assess flexibility of a large scale implementation. To address this shortcoming, a change in feedstock with significantly different bio-oil yield was conducted in the bioliq® pilot unit that was designed for a feedstock capacity of 500 kg h^{-1} wheat straw. Miscanthus was used in two experimental campaigns that each lasted two weeks. While steady state operation succeeded, feedstock capacity had to be reduced significantly to around 200 kg h^{-1} to allow for a better control of pressure fluctuations in the hot gas section. An evaluation of volume flow rates reveals that these fluctuations are not due to an increased volatile yield. It is concluded that plugging issues caused by an increased reactivity of the produced volatiles likely caused the observations and limitations to plant capacity. The heat demand to operate the fast pyrolysis unit was estimated to be 0.8 to 1.5 MJ kg^{-1} for both miscanthus campaigns and 0.6 to 1.1 MJ kg^{-1} for wheat straw. The high uncertainty associated with these values is based on limited precision to determine the heat carrier mass flow and likely underestimates the true value. The yield distribution from miscanthus has been compared to experiments conducted in parallel in a smaller process development unit with a feedstock capacity of 10 kg h^{-1}. The results impressively show the influence of ash content on the yield distribution and also the importance to focus on (earth) alkali metals to better describe their catalytic activity during biomass pyrolysis. Finally, water content as one important product characteristic of the produced bio-oil has been modelled for the applied condensation temperatures and compared to experimental results.

Keywords: Fast pyrolysis, Miscanthus x giganteus, bio-oil, operational experience

1 Introduction

Bioenergy is considered an important pillar of decarbonisation in the energy transition as a near zero- and even a negative emission fuel. Advanced bioenergy applications contribute to around 7 % of the primary energy consumption today [1]. Bioenergy is even more useful because it can be flexibly used in different energy sectors providing solid, liquid and gaseous biofuels for electrical power and heat in homes and industrial plants as well as liquid biofuels used in the transportation sector. In many cases, it can benefit from existing infrastructure in production, distribution and application.

In Europe, the discussion on competing biomass uses and future supply has led to criteria for sustainable biomass supply for bioenergy applications [2]. In the first line, the biomass used should not compete to food or animal feed production. Also, the used biomass should not be needed to maintain ecological functions, such as soil humus content (agriculture) or to replace nutrient withdrawal by harvested woods (forestry). Finally, the biomass should be grown on marginal land, which is land not suitable or economically attractive for food crop production [3]. With these prerequisites, biomass for bioenergy is limited to wood, by-products and residues from agriculture and forestry, and purpose grown plants cultivated on marginal land.

Apart from its use as a material, wood is already widely utilized for bioenergy production mainly by combustion utilizing traditional (heating) and advanced technologies (combined heat and power), but also by other thermochemical conversion processes such as pyrolysis or gasification to produce intermediate energy carriers for further fuel or chemicals production. Wood, in general, is an intensively used resource and harvest intensity cannot be much increased without negative effects on the forest ecosystems. However, residues of forestry and agriculture may be used to a larger extent. However, parts of it are required to maintain humus content and soil fertility as well as for other applications [4]. For agricultural applications, it is estimated that roughly 40% of agricultural residues need to remain on the field [5]. The amount of unused agricultural and forestry residues available is still significant and opens up interesting additional potential for bioenergy applications – apart from modernizing existing energy uses [6]. In addition to existing wood resources, agricultural and forestry residues and by-products, a future, large potential for lignocellulosic biomass production is seen in the cultivation of dedicated perennial biomass crops (PBC) on agricultural land that is not needed or suitable for the cultivation of food crops. However, the actual availability of marginal land in Europe shows a broad range depending on the assumptions made, varying from 53.600 out of 300.000 km^2 of available marginal land up to 388.000 km^2 out of 647.000 km^2 , respectively [7,8].

To grow perennial crops, land-use change occurs, but with potential positive effects. For example, greenhouse gas emission can become beneficial when perennial biomass crops replace annual crops and lead to carbon accumulation in soil [9]. In perspective, these plants could even be cultivated as intermediate crop within carbon-farming approaches for soil recovery purposes. Among the different lignocellulosic energy plants suitable for this purpose that show beneficial characteristics for thermochemical conversion, miscanthus is one much discussed and already applied option. *Miscanthus X giganteus* is the predominant genotype cultivated in Europe. It is a low input crop with high nitrogen, land-use and energy efficiency [10]. After an establishment period of at least two years, it can be harvested annually over around 20 years of cultivation time. On good arable land, dry matter yields of around 26 t ha^{-1} yr^{-1} can be obtained in Germany. Depending on the genotype, the conditions and location of cultivation, harvest yields differ significantly in EU ranging from 4 t ha^{-1} yr^{-1} (values below

appear unlikely to occur in practise up to 40 t ha^{-1} yr^{-1} under optimum conditions [10,11]. Scenarios made up to estimate the possible miscanthus potential usually make use of a mix of different types of spatially distributed land quality and, thus, harvest yield. A study dedicated to the production of industrial heat from giant miscanthus combustion in France, for example, made use of 3.3 Mha of marginal lands (ca. 6 % of its continental territory) considering harvest yields above 11 t ha^{-1} yr^{-1} providing a yield of 37.6 TWh yr^{-1}. Assuming a gross calorific value of 19 MJ kg^{-1} this would mean around 7 Mio. t of dry biomass [12]. Production costs varied from 28 EUR t^{-1} to 67 EUR t^{-1} with a weighted average of 38 EUR t^{-1}.

Regarding the multitude of feedstocks available for future bioenergy applications, conversion technologies need to tackle two goals at the same time: on the one hand, they should allow to be fed with different feedstocks (separately or in mixtures) and on the other hand, the obtained products need to meet certain specifications demanded by their further usage. While the use of wood in combustion, gasification and pyrolysis can be considered state-of-the-art, the use of other types of biomass, except for combustion, is not that common. Fast pyrolysis appears as an excellent choice to decouple biomass production from bioenergy use in place and time. The main product of fast pyrolysis is liquid bio-oil (FPBO, fast pyrolysis bio-oil), produced from wood and used as heating oil with production capacities of up to 50,000 t yr^{-1} per plant today [13]. Current research and development aim at the use of FPBO as refinery feedstock as it is or after catalytic hydrotreatment, or as gasification fuel for synthesis gas production and downstream conversion to synthetic fuels and chemicals. An overview of the current state of the art in fast pyrolysis regarding process fundamentals, technologies, and feedstocks, as well as product yields and properties is given in the comprehensive reviews [14-16] containing a valuable list of references.

There is a gap between today's commercial application of fast pyrolysis for liquefaction of wood and the anticipated extension to residual feedstocks which often also have high ash content. While in laboratory and bench scale different types of biomass have been thoroughly investigated in terms of product distribution, yields, and composition [17,18], there is much less reporting on the practical experience of pilot plants utilising different feedstocks. The objective of this study is to identify limitations of an existing fast pyrolysis unit in relevant scale when changing the type of feedstock to get a better picture of the flexibility in operation once steel has been put into the ground. One important aspect of this study is long-term operation of such a plant (i.e. several days as compared to several hours in laboratory scale). Hence, this study presents the results of two test runs with giant miscanthus in the bioliq® fast pyrolysis pilot plant with around 300 kg h^{-1} feed capacity which was originally designed for and operated with wheat straw as feedstock [19]. In parallel, experiments have been conducted in a 10 kg h^{-1} process development unit with similar setup to allow for comparison with a more common research scale.

2 Materials and Methods

2.1 Pyrolysis plants

The same miscanthus material was first used in the process development unit (Python) and afterwards in the bioliq® fast pyrolysis plant. Figure 1 shows a flowchart of the bioliq® plant [19]. A twin screw mixing reactor is used for the pyrolysis reaction. For rapid heat transfer, hot sand as heat carrier enters the reactor first, than biomass is added up to 500 kg/h. To make sure that oxygen does not affect the reaction, nitrogen is supplied as inert gas. Reaction takes places at atmospheric pressure. The heat carrier temperature is measured when leaving the reactor from underneath and is maintained at 500 °C. Produced gases and vapours from fast pyrolysis reaction entrain fine char particles, which are separated in the product gas cyclone.

A certain amount of the produced char is carried over with the sand in the heat carrier loop, where the heat carrier is recirculated and reheated with hot flue gas generated in a gas burner. By controlling the oxygen excess in the flue gas, the char entrained into the heat carrier loop is combusted in the lift pipe to provide additional heat before the sand re-entering the reactor. Combustion gases containing fine particles are treated in the flue gas section of the plant. After passing the cyclone, pyrolysis gases and vapours are instantly cooled down in two sequentially arranged loops. At first, vapours are condensed at 90 ± 5 °C, which yield organic rich condensate (ORC). This ORC would be commonly referred to as FPBO in a single stage condensation. The second loop has a condensation temperature of 25 ± 5 °C where the aqueous condensate (AC) is obtained. Non-condensable gases are subsequently detected by a gas chromatograph and flared. Calculations show that the so produced heat could potentially be used internally to sustain the process as in commercial fast pyrolysis units, which is not realized in the current pilot plant setup to ease operation [19].

The smaller fast pyrolysis process development unit (Python, 10 kg h^{-1}) is based on the same principle with a scale down factor of 50. A detailed flow diagram of the experimental setup of the Python unit and the experimental procedure is described elsewhere [20]. In Table 1 the plant settings and differences between both plants are depicted. Main differences of both plants relate to the layout of the heat carrier loop. In the Python plant 1 mm steel beads are used as heat carrier, which are recirculated with a bucket elevator and reheated electrically in a heat exchanger. Inversely to the pilot plant, in the Python unit biomass is fed into the reactor first and then heat carrier drops onto the moving bed of biomass.

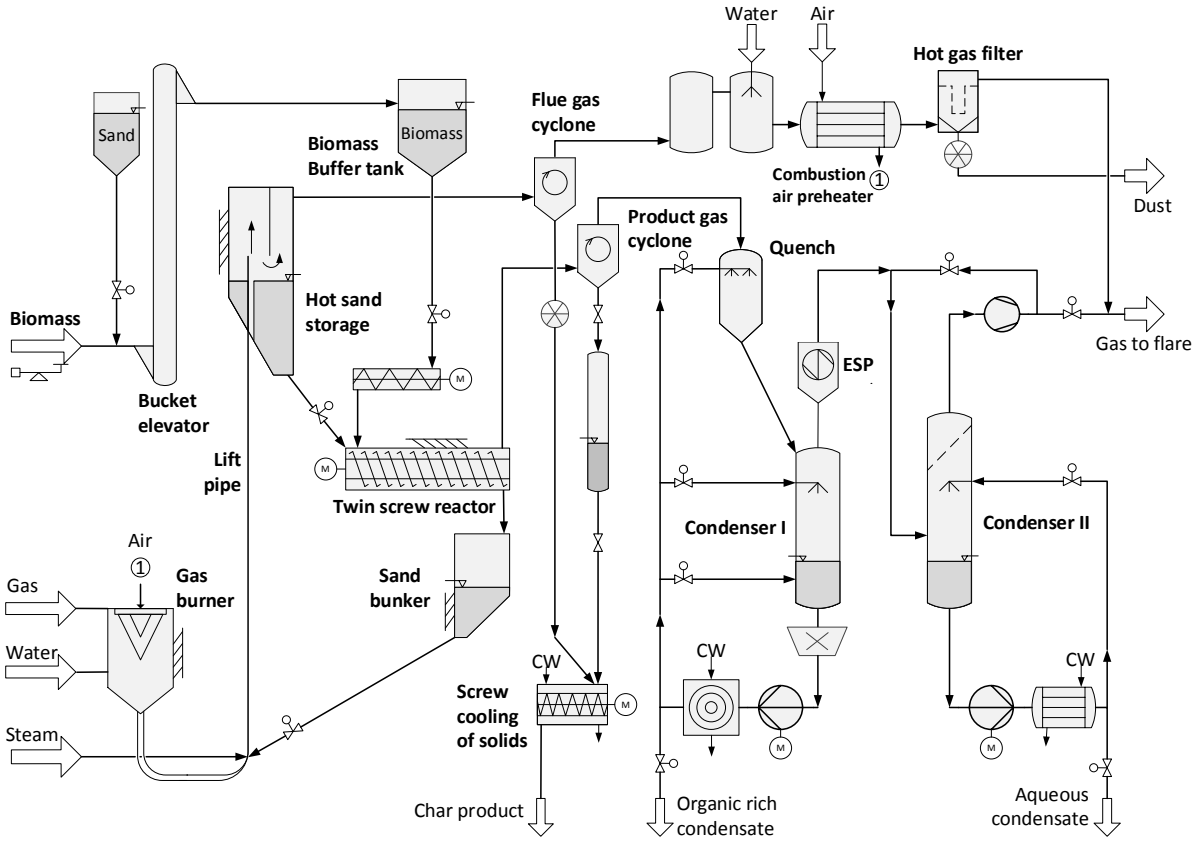

Figure 1: Flowchart of the bioliq® pyrolysis plant

Table 1: Plant settings of the bioliq® and Python pyrolysis plants

		bioliq® pyrolysis	Python
1. Feed capacity	kg h^{-1}	500	10
2. Heat supply			
2.1. Heat carrier loop			
2.1.1 Material/ size		Quartz sand 1-1.7 mm	Spherical steel particles 1 mm
2.1.2 Heat source		Burning chamber (gas), also burning of char particles (from pyrolysis process)	Heat exchanger (electric)
2.1.3 Material transport		Pneumatic lift lift gas from burning chamber	Bucket elevator
2.1.4 Material consumption		Losses by abrasion, refill (200-1000kg/experiment)	-
2.2 Reactor			
2.2.1 Type		Twin screw mixing reactor	
2.2.2 Feeding array		First: heat carrier then: biomass	First: biomass then: heat carrier
2.2.3 Reactor temperature[a]	°C	500	500
2.2.4 Reactor pressure		Atmospheric	
2.2.5 Gas phase retention time	s	1-2	~1
3. Product separation			
3.1 Particle separation		1 cyclone	2 cyclones in series
3.2 Condensation step 1			
3.2.1 Setup		Quench, condenser and electrostatic precipitator, macerator, pump, heat exchanger	
3.2.2 Temperature[b]	°C	85-90	90
3.3 Condensation step 2			
3.3.1 Setup		Condenser, heat exchanger, pump	
3.3.2 Temperature[b]	°C	20-30	20
3.4 Gas treatment		Burned in flare	Vented
4. Pressure regulation		Blower	

[a] Measured at heat carrier outlet [b] Measured at of condenser bottom

2.2 Feedstock

In total, 260 tons of wheat straw have been pyrolysed in the bioliq® pyrolysis plant since 2012 in 9 test campaigns and operational experience was gained during a cumulative operational time of 740 h. After many years of utilizing wheat straw as feedstock for the fast pyrolysis process in the bioliq® plant, giant miscanthus was chosen as feedstock to test flexibility of the installation. Table 2 compares the characteristics of miscanthus and wheat straw.

Table 2: Comparison of wheat straw and miscanthus x giganteus

	Wheat straw	Miscanthus
Scientific name	*Triticum*	*Miscanthus x giganteus*
Type	Annual Poaceae, C_3-crop	Perennial C_4 crop
Life	Sowing in autumn or spring, harvest in summer	2 – 3 years to reach full production potential and has a stand life of about 15 - 20 years
Fertilizer	Nutrient supply necessary: first nitrogen supply end of winter , second in April, third in June	Mainly on Soils with low N contents, maximum 50 - 70 kg N ha^{-1} yr^{-1},nutrient requirement: 0.3-1.1 kg phosphorus and 0.8-1.0 kg calcium per $t_{dry\ matter}$ [21]
Harvest	Summer	Single harvest late in the fall or early spring before new shoots emerge, low mineral contents, moisture content of less than 15%
Availability	In the EU, about 144 million tonnes harvested each year [22] In Germany, 10-16 million dry tonnes per year, of which 4 million tonnes already find material use and almost none energetic use [6]	- In Germany: around 26 t/(ha yr) - In EU: 4 t/ha yr up to 40 t/(ha yr) [10]
Application	Material and energetic use: - Agricultural use (as source of humus and nutrients in soil of agricultural areas) - Bedding /animal husbandry - Building and isolation material - Paper industry [23,24]	Wide range of utilization pathways including combustion, conversion to bioethanol, production of building materials and of basic chemicals [25]

The wheat straw used so far was delivered and used in large square bales (approx.: 2500x1300x750 mm; 350 - 400 kg), which are fed to the milling system separately by a forklift. Also Miscanthus could be purchased in form of bales; therefore, biomass preparation did not required a change in the milling and feeding system used: Chopping of the bales first in a shredder and then in a cutting mill, pneumatic transport of the ground material, its storage in a silo and feeding to the pyrolysis reactor were possible with the existing equipment. The first batch of miscanthus was provided by a farmer in Bavaria (Biohof Aufmuth, Ruderatshofen), supplying 18.5 tons of miscanthus (Miscanthus #1). More of the same material was not available for the second test campaign, so that an additional, second batch was organized from Miscanthus Falzberger, Pichl bei Wels, Austria (Miscanthus #2). As a result, Miscanthus #1 was used in the campaign in 2019 whereas the remaining Miscanthus #1 and new Miscanthus #2 were pyrolysed in 2021 (mass ratio approx.: $\frac{Miscanthus\ \#2}{Miscanthus\ \#1} \approx 4$). In the Python plant, the batches were used separately. Analyses of the two miscanthus batches are summarized in Table 4.

2.3 Methods

Mass balances for the bioliq® and Python pyrolysis plants were established. For a description of the detailed methods, measurement points in the plants and data provided for balances from each experiment see [19] and [20].

To calculate the expected water content in the organic-rich condensate as a function of condensation temperature, surrogate mixtures for FPBOs were generated from its compositional data. The selection of surrogate compounds followed a similar principle as published elsewhere [26] such that it covers the boiling range of present individual components and all relevant functional groups are represented. The mass fractions of selected surrogate compounds in the pyrolysis vapours that enter the first condensation

stage were estimated using the respective mass fractions of these components in the ORC and AC as well as the product yield of all streams of the condensation setup. GC-undetectable compounds present in the ORC were represented as 3,4,4'-Biphenoltriol. Vapour-liquid equilibrium flash calculations were executed using the UNIFAC-DMD model in ASPEN Plus version 12, with the condensation stage modelled as a flash column.

For analysis of the educt and the product materials, standard methods as compiled in Table 3 were used. Milling of biomass samples prior to analysis was done with cryomill Freezer/Mill 6875 from SPEX SamplePrep.

Table 3: Overview of equipment and standard methods applied for analysis

		Equipment	Standard
Solids	Water (solids) content	Leco TGA701	DIN EN ISO 18134-3
	Ash content	Leco TGA701	DIN EN ISO 18122
	C,H,N content	LECO CHN 628	DIN EN ISO 16948
	Minerals and micro elements		DIN EN ISO 16968
Liquids	Solids (liquids)		ASTM D 7579, modified
	Water (liquids)	Metrohm Titrando 841	ASTM E203, modified
	Density	Anton Paar DMA 4500 M	DIN EN ISO12185
	Viscosity	Anton Paar MCR 102	Internal method
	PH	Metrohm 827 pH lab	DIN EN ISO 10523
	Total organic carbon (TOC)	Dimatec Dimatoc 2000	DIN EN 1484
	Chemical oxygen demand (COD))	Hach Lange DR 3900	DIN ISO 15705
	Higher heating value (HHV)	IKA C5000 bomb calorimeter	DIN EN 14918
Gas	CO, CO_2	Emerson Gas chromatograph Daniel Modell 700	

Biomass samples were taken periodically during operation of the two pyrolysis plants. Due to observed reproducibility issues, analyses were performed on ground and unground samples. Each sample was analysed in triplicates and homogeneity was satisfactory with low deviations.

Selected samples (steady-state operation) of organic rich condensate (ORC) and aqueous condensate (AC) were sent for quantitative and qualitative analysis to Thuenen Institute (Hamburg, Germany). Compounds were detected and quantified in a gas chromatograph (HP 6890) with two parallel detectors (FID and MS (HP 5972)). Detailed information to the method applied can be found in Windt et al. [27]

3 Results

3.1 Biomass analysis

Average analysis results of miscanthus as used in the bioliq® and Python trials are summarized in Table 4 and Table 5. It was observed that the second miscanthus batch is characterized by a very high ash content and heterogeneity as compared to the first one. Within experimental uncertainty, water and ash content show similar results between the bioliq® and Python test runs.

Table 4: Overview of feedstock characteristics

	Miscanthus #1 2019[d]	Miscanthus #2:#1 4:1 2021	Miscanthus #1 (Python)	Miscanthus #2 (Python)
Water content (wt %, ar[a])	9.4 ± 0.5	8.4[e] ± 0.2	10.2 ± 0.1[g]	8.7 ± 0.3[g]
Ash content (wt %,dry)	2.4 ± 0.8	9.5[e] ± 1.1	2.2 ± 0.1[g]	11 ± 3.5[g]
Elemental analysis (wt %,dry)				
C content	48.4	44.4[f]		
H content	5.7	5.4[f]		
N content	<0.3	0.5[f]		
O[c] content	43.3	40.3		
HHV (MJ kg^{-1}, dry)[b]	19.1	17.4		

[a] As received [b] By difference [c] Calculated (Channiwala) [d] Number of samples n=10 [e] Number of samples n=14; milled [f] Number of samples n=7; milled [g] Number of samples n=3-4

As obvious from Table 4, the ash content observed during the bioliq® test campaign in 2021 is four times higher than that of the bioliq® campaign in 2019. Literature [17,28] and an online biomass data base [12] report an ash content for miscanthus of about 1.5 - 5 wt % on dry basis. Compared to these literature values, miscanthus used in the bioliq® process 2021 is obviously characterized by an unusually high ash content. Therefore, location, harvesting time and other influencing parameters were checked. Miscanthus #1 was harvested in spring 2019 after snowmelt and Miscanthus #2 in May 2020. Miscanthus #1 was cut 8 cm above the ground by a double blade mower, afterwards a hay rake and baler were used for collection. Miscanthus #2 was cut with a device for mulching (flail mower approx. 20 cm above ground, leaves were included). Afterwards also a hay rake and baler were used. Leaves have a higher ash content than the stem [29,30]. Comparing the analyses of the inorganic material of 7 individual samples (see Table 5), specific elements such as e.g. silicon increase proportionally to the ash content while others do not. Silicon content is probably related to intake of sand from soil during harvesting. It is also possible that waste, such as tins, could be mulched with the biomass and affect these results (higher aluminium and iron contents) due to the location of the field. The large difference in the ash content enabled an investigation on the pyrolysis plant and product behaviour with a significant change of the feedstock composition.

Table 5: Elemental analyses of miscanthus samples

			Miscanthus #1			**Miscanthus #2**	**Miscanthus #2:#1 4:1**		
Sample number			**1.1**	**1.2**	**1.3**	**2.1**	**2.2**	**2.3[a]**	**2.4**
Ash content		**wt %, dry**	**2.2**	**3.0**	**4.2**	**10.5**	**11.2**	**20.1**	**8.4**
Aluminium	Al	mg kg^{-1}	240	588	915	3313	4192	9213	2872
Calcium	Ca	mg kg^{-1}	1967	1811	2860	1754	2724	3589	1785
Iron	Fe	mg kg^{-1}	214	497	767	2656	3242	6705	2175
Potassium	K	mg kg^{-1}	1687	1727	2015	3313	3918	4806	3442
Magnesium	Mg	mg kg^{-1}	1118	937	1232	1497	1468	2560	1130
Manganese	Mn	mg kg^{-1}	24	45	62	117	140	244	108
Sodium	Na	mg kg^{-1}	< 10	< 10	< 10	113	129	238	95
Phosphorus	P	mg kg^{-1}	503	496	675	452	567	674	504
Sulphur	S	mg kg^{-1}	255	354	399	613	464	625	344
Silicon	Si	mg kg^{-1}	1553	2144	2182	31487	42344	69045	27983
Titanium	Ti	mg kg^{-1}	< 10	17	25	117	121	302	114

Total halide content Cl, Br, I (excl. F)	mg kg^{-1}	217	185	188	1005	636	614	283

[a] This sample is an outlier and is not considered in the following evaluation

3.2 Operational experience

In 2019, biomass intake into the bioliq® pyrolysis reactor was operational for 68 h and 2021 for 104.5 h (i.e. operational time excluding interruptions). In 2020, no pilot plant operation took place.

During the pilot plant test campaign in 2019, nine interruptions required a stop of feed dosage. Those were mainly caused in the first half of the campaign by too large pressure fluctuations induced by the acoustic cleaning unit (safety shutdown at defined pressure). It cannot be concluded whether the pressure increase is due to new feedstock, different time or continued operating of the cleaning device or simply due to a lack of operating experience with the new feedstock. By adapting the operation mode of the acoustic cleaning system, it was possible to continue its use without interrupting the process again. In the second half of the operation time, the experiment was interrupted due to bridging of miscanthus material in the biomass buffer tank before the reactor. The interruptions lasted a few minutes in each case and biomass flow was quickly re-established again. At the beginning, the biomass feed rate was adjusted to around 300 kg h^{-1} for about 24 h. Afterwards it was reduced to around 200 kg h^{-1} due to the increased pressure losses. This reduction in feed supply allowed for stable operation. Longest operation without interruption was 19 h.

In the 2021 pilot plant campaign, the biomass flow was stopped 11 times due to varying problems: operating errors, auxiliary equipment failure (but which could solved during the campaign), problems owing to deposits in product line (cleaning unit got stuck in quench) and bridging of biomass material in the biomass buffer tank (same as in 2019). Longest period of biomass feeding in 2021 without interruption was 58 h with an average feeding of about 200 kg h^{-1}.

Both miscanthus batches were pyrolysed in the Python pyrolysis plant without any significant issues during operation.

3.3 Yields

Figure 2 shows the mass yields of the bioliq® and Python plant for miscanthus and the previous wheat straw runs on an as-received basis. The product char includes char recovered from the process and the fraction spent in internal combustion (through calculations). Solids contained in the ORC are reported separately; hence, the ORC yield is presented as the product from the first condenser without solids. This is important to note since the ORC produced in the bioliq® plant contains significant amounts of char fines due to the concept of the bioliq® process, which does not require a solid-free bio-oil for its gasification and subsequent production of synthetic fuels [31].

Results from wheat straw conversion in the bioliq® plant have been reported previously [19]. Unpublished results have been taken from the Python plant operation; five representative experiments have been chosen to define a base case (similar feeding and condensation temperatures) for comparison purposes in this study.

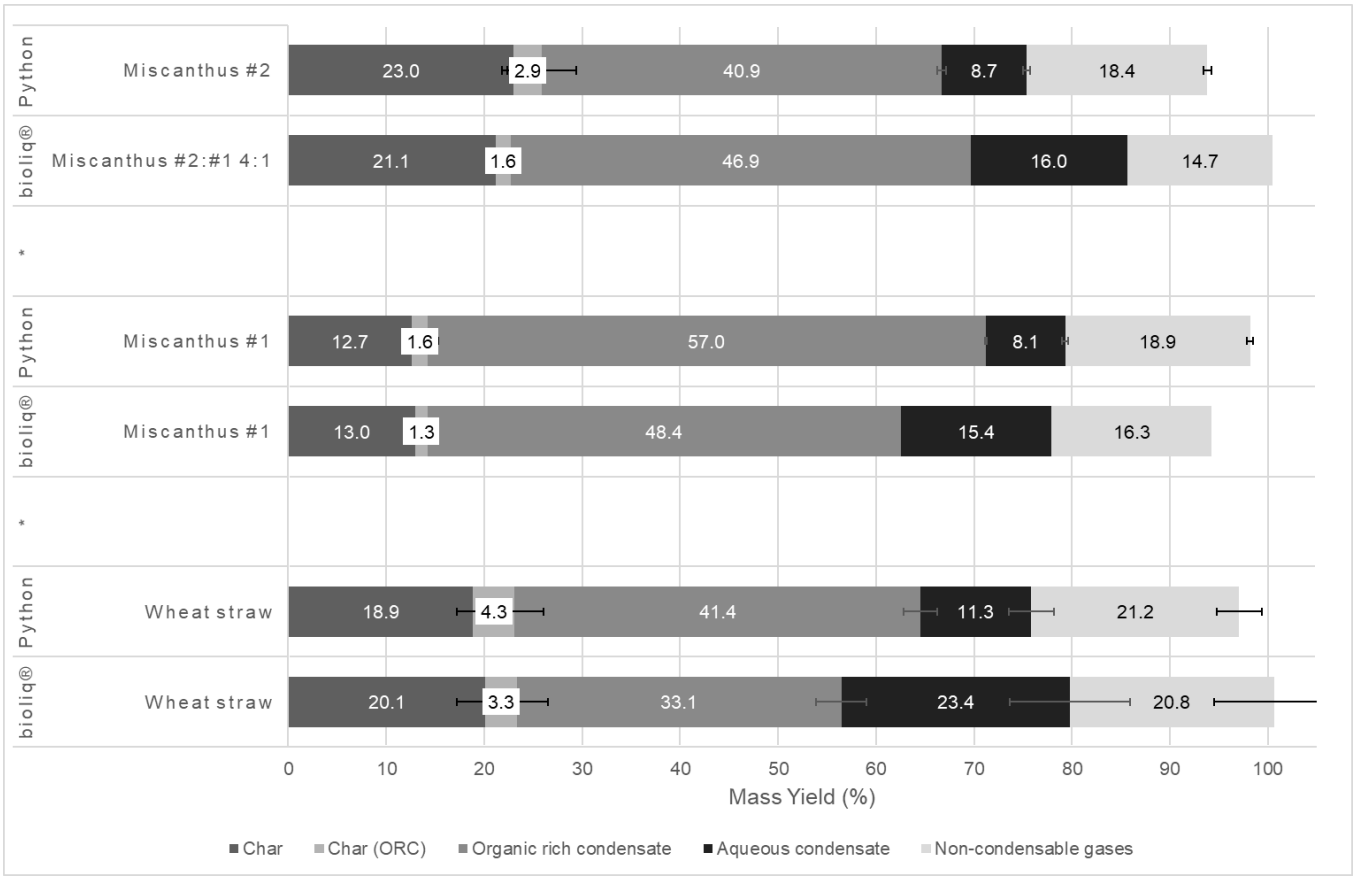

Figure 2: Overview on mass balances of miscanthus experiments at bioliq® and Python (as received basis of feedstock and products); due to only one test performed, no standard deviation for bioliq® miscanthus is specified

The liquid yields (sum of ORC and AC yields) for the fast pyrolysis of miscanthus in the bioliq® plant are higher with 62.9 wt % (Miscanthus #2:#1 4:1) and 63.8 wt % (Miscanthus #1) compared to those of straw (56.5 wt %). The yields for AC are higher and the yields for ORC are lower for wheat straw. Results for the formation of reaction water (on dry base) are 13.1 ± 0.5 wt % for miscanthus and 17.7 ± 1.3 wt % for wheat straw. In 2021, there was a slight excess of yields and 2019 a deficit. Another noticeable difference of yields can be observed in the formation of char. Miscanthus #2 leads to production of more char than straw and Miscanthus #1. The same trend is also found in the results of the Python plant. Correspondingly, less ORC and AC is received.

The organic liquid yield (OLY) comprising of the combined mass of all organic substances from organic rich and aqueous condensate and excluding solid contents is compiled in Table 6. Interestingly, there is little difference between the OLY obtained from the two miscanthus batches in the bioliq® plant, especially compared to the significant drop in OLY observed in the Python plant product.

Table 6: Comparison bioliq® pyrolysis and Python with miscanthus as feed

	Campaign	Total feed	Average feed rate	OLY
		kg, ar	kg h^{-1} ,ar	%
bioliq®	2019	14692	212	47.8
	2021	18169	174	46.9
Python	2019[a]	20	5.8	51.2 ± 0.7
	2021[b]	20	5.5	36.7 ± 3.2

[a] Average of 2 experiments [b] Average of 3 experiments

3.4 Product properties

Generally, the products of both campaigns at the bioliq® plant appear to be quite similar. In Table 7 , the product properties of the products are compiled for comparison. Practically no difference is noted in viscosity of the ORC as well as in the composition of solid products. The solid content in ORC is slightly higher in 2021 while a more significant difference occurs in the content of inorganic material, which is about three times larger in the ORC in 2021. The char produced in 2021 also contains much more inorganic material, also reflected in the significantly lower HHV.

Table 7: Properties of products (as received) during miscanthus pyrolysis at bioliq®

Property	Dimension	2019	2021
		Organic rich condensate (ORC)	
Water content	wt %	14 ± 4[a]	13 ± 4[e]
Solid content	wt %	3 ± 1[a]	5 ± 2[e]
Inorganic material	wt %	0.3 ± 0.1[b]	1.6 ± 0.1[b]
Density (20 °C)	kg m^{-3}	1235 ± 15[b]	1235 ± 40[f]
Viscosity (80 °C)	mPa s	20 - 80[a]	20 - 220[e]
Homogeneity		homogeneous	homogeneous
HHV	MJ kg^{-1}	20.6 ± 0.7[b]	21 ± 1[1,f]
C content	wt %	50 ± 2[b]	48 ± 5[f]
H content	wt %	7.0 ± 0.2[b]	7.1 ± 0.6[f]
N content	wt %	0.3 ± 0.1[b]	0.4 ± 0.2[f]
		Aqueous condensate (AC)	
Water content	wt %	82 ± 3[c]	82 ± 3[g]
pH value	-	2.2 ± 0.1[b]	2.3 ± 0.3[f]
Density (20 °C)	kg m^{-3}	1016 ± 1[b]	1011 ± 8[f]
HHV[1]	MJ kg^{-1}	3.4 ± 0.3[b]	3.5 ± 0.5[h]
TOC	mg L^{-1}	90000 ± 5000[b]	85000 ± 7000[f]
COD	mg L^{-1}	233000 ± 25000[b]	259000 ± 18000[f]
		Solid char product	
Mineral content	wt %	21 ± 2[d]	52 ± 9[i]
HHV	MJ kg^{-1}	24 ± 1[1,d]	14 ± 3[1,i]
C content	wt %	66 ± 2[d]	40 ± 8[i]
H content	wt %	2.3 ± 0.1[d]	1.7 ± 0.2[i]
N content	wt %	0.9 ± 0.1[d]	0.8 ± 0.1[i]

[1] calculated (Channiwala)
number of samples: [a] n= 36 ; [b] n=5 ; [c] n=12 ; [d] n=6 ; [e] n=60 ; [f] n=4 ; [g] n=22 ; [h] n=3; [i] n=8

The viscosity is dependent on operating parameters and composition of the ORC. In both campaigns, there is a constant increase of viscosity in steady state operation: up to around 40 mPa s in 2019 and 50 mPa s in 2021. Due to interruptions of the process and less water in ORC there is a sudden increase in viscosity. In 2021, the viscosity promptly increases to 220 mPa s as the process was interrupted for a few hours and the condensation loop was only operated periodically. When pyrolysis was continued, viscosity went back to values between 100 to 150 mPa s.

4 Discussion

4.1 Biomass diversity and sampling

Location, pretreatment, method and date of harvest are important factors determing biomass properties and their following conversion. Changes in these parameters can significantly affect conversion yield and product characteristics. Between the results (mass balances) of the two miscanthus experiments, large differences were noticed. One obvious reason can be found in the high deviation of the ash content between the two miscanthus batches (see Table 4) which will be further discussed below during comparison of yields from the bioliq® and Python plant.

It was also observed that Miscanthus #2 with its high ash content is characterized by a higher heterogeneity during sampling. This is a commonly observed phenomenon with ash rich biomass, especially if the high ash content is attributed to an increased contamination with soil. Soil tends to contain much smaller particles and hence agglomerates in the bottom during handling and storage. This leads to a large spatial differences of cut feedstock piles and directly affects the interpretation of the mass balance due to the increased difficulty to obtain representative samples along the operation time of a campaign with in total 15-20 t input material. Sampling of biomass feedstock (approx. 100-200 g each) was conducted manually from the conveyor belt six times an operational day (i.e. 24 h) and two were combined to yield one sample per shift. This combined sample was then divided in an automated sampling apparatus prior to analysis. While this procedure proved to be sufficient for largely homogeneous feedstock samples, it is clear that it must become inaccurate for the Miscanthus #2 batch due to its exceptionally high heterogeneity.

4.2 Operational conditions

Figure 3 shows the startup period for Miscanthus #1 in 2019 and wheat straw pyrolysed in 2017. This specific wheat straw campaign was chosen because its start-up procedure is similar to that of the miscanthus campaign. The pressure drop over the hot gas section, i.e. between pyrolysis reactor outlet and inlet of the gas blower located behind the second condenser, is compared for these campaigns. It is shown together with the biomass feed rate; however, complete interruptions of the biomass dosing and partly start-up phases are not shown to improve readability. During the miscanthus campaign pressure loss rose quicker and remained at a higher level. It was decided to reduce the biomass feed rate which led to a decrease in pressure drop and stable operation. Reductions of the biomass dosing show that the pressure is strongly dependent on the feed rate, well visible at minute 1500 for the miscanthus campaign. For the miscanthus campaign in 2021 the pressure drop was also in the range as the one observed during wheat straw pyrolysis but the feed rate has been set at 200 kg/h right from begin of operation.

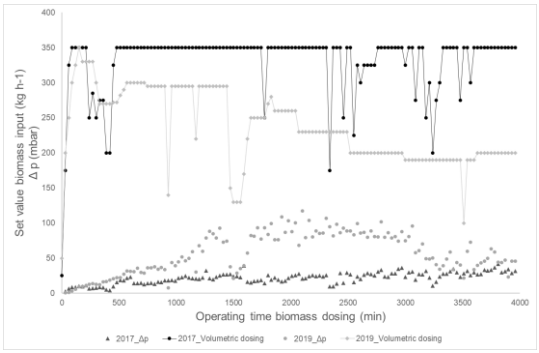

Figure 3: Comparison of pressure increase and volumetric dosing in the start-up period of the 2017 wheat straw and the 2019 miscanthus campaigns

The observed pressure difference increase during operation with miscanthus has not been detected to this extent during previous runs with wheat straw. One explanation could be an increased volume flow rate, which can expected at the lower char yields because all other pyrolysis products significantly add to the volume flow at reactor temperature. The volume flow at reactor outlet (at 500 °C and 1 atm) is directly dependent on biomass input (see Figure 4). The volume flow includes inertisation gas (nitrogen – constant input independent of biomass input), steam (from biomass-moisture and reaction water formed during pyrolysis), and organic vapours after biomass pyrolysis in the twin screw reactor.

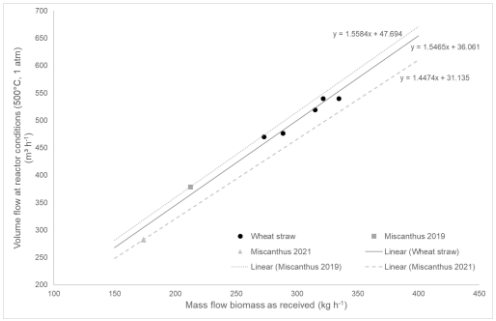

Figure 4: Calculated volume flow rate including inertisation gas, steam, pyrolysis gas and vapours, as a function of biomass input

To allow for a better comparison of the volume flow rate during the different experimental campaigns based on different yields and feeding rates, the expected flow rate for each feedstock was calculated as a function of the feeding rate. The resulting linear correlations for Miscanthus 2019, Miscanthus 2021, and average results of previous wheat straw campaigns (2015-2018) are shown in Figure 4. The different slopes represent the average volatiles yield during pyrolysis (i.e. difference between char yield and biomass fed).

At same biomass feeding rate, Miscanthus 2019 shows the highest volume flow rate, followed by wheat straw and Miscanthus 2021. It can also be observed that the volume flow rate during previous wheat straw campaigns was significantly higher than during both miscanthus campaigns (470-540 m³/h and 300-350 m³/h, respectively). It follows that the lower feeding rate during miscanthus campaigns counteracts the higher volatiles yield. It is concluded that the observed pressure fluctuations do not originate from a higher volume flow.

Nevertheless, it was observed during miscanthus campaigns that pressure fluctuations were less problematic at lower miscanthus feeding rates. It is known that over the time of each experiment deposits are formed consequently causing a pressure increase. After experimental campaigns, pipelines were inspected and cleaned. Deposits found had a

layered structure. The observations during wheat straw and miscanthus campaigns hint to a different extent of such depositions. It is hypothesized that it increases with reactivity of liquids contacting the surfaces, and that this reactivity is higher for feedstocks with lower ash content due to less heterogeneous catalytic effects in the hot vapour phase. Since the miscanthus feed rate was significantly lowered to reduce pressure fluctuations, these effects represent an important limitation in terms of plant flexibility to feedstock changes.

The heat energy required for maintaining a constant reaction temperature of ca. 500 °C during fast pyrolysis of biomass is of interest for a proper plant design. It is important to get an indication for data at scale since geometry and industrial plant design (piping insulation etc.) significantly affect the energy requirements. At the same time, carefully controlled conditions are more difficultly obtained as compared to laboratory setups.

The most viable option for the calculation of the heat demand for heating and pyrolysis of biomass in the reactor including thermal losses is by considering the heat carrier entering and leaving the reactor. The amount of heat transferred in the reactor by the heat carrier is the product from $\Delta T_{heat\ carrier}$ (temperature of heat carrier above gate valve before entering reactor minus temperature of heat carrier after leaving the reactor), with $c_{P,\ heat\ carrier}$ as specific heat capacity of quartz sand at measured temperature and the mass flow of heat carrier $\dot{m}_{\ heat\ carrier}$ before entering the reactor. For a more detailed description of the energy balance and calculation pathway see Henrich [32].

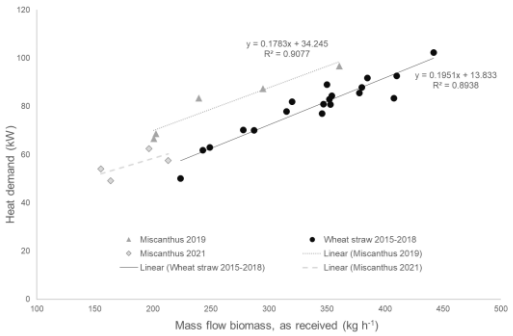

Figure 5: Heat demand for the reactor (including heat losses) for wheat straw and miscanthus campaigns for varying mass flow rates.

Figure 5 shows results of this calculation for various steady-state periods during the wheat straw campaigns 2015-2018 and miscanthus campaigns 2019 and 2021.

The data for wheat straw and Miscanthus 2019 can be fitted reasonably well by a linear trend line with an R^2 of around 0.9. These trends indicate a constant specific heat demand for pyrolysis, i.e. heat demand per mass unit of biomass (kJ kg^{-1}), and a constant heat loss via thermal insulation independent of the biomass feed rate between 150 and 450 kg h^{-1}. For Miscanthus 2021 only 4 data points during steady-state operation are available with a relatively high variation and a relatively narrow mass flow range (between 150 and 215 kg h^{-1}), which is below or just within the lowest mass flow range of the previous campaigns.

The mean specific heat demand of miscanthus campaigns 2019 and 2021, 1.14 ± 0.12 MJ kg^{-1} and 1.10 ± 0.12 MJ kg^{-1}, respectively, is significantly larger than that for the mean of wheat straw campaigns of 0.85 ± 0.05 MJ kg^{-1}.
This is in line with the observation that an increase in organic liquid yield is associated with an increase in reaction enthalpy and thus an increase of the heat demand inside the reactor [33]. It is also noted that there is a high deviation of the above-calculated values compared to

data published elsewhere. Henrich [32] and Daugaard [34] report a broad range of specific heat demand of various types of biomass like ca. 0.78 ± 0.20 MJ kg^{-1} (oat bran), 1.25 ± 0.30 MJ kg^{-1} (wheat straw), or 1.96 ± 0.42 MJ kg^{-1} (softwood) on a dry basis. For wheat straw with a typical as-received water content of 9 wt % as used in the bioliq® experiments the heat demand increases to ca. 1.44 ± 0.27 MJ kg^{-1}. These values represent only the heat demand for pyrolysis, not including any heat losses. It becomes obvious that calculations for the heat demand obtained from the experimental setup of the bioliq® campaigns is leading to a significant underestimation.

The main source of uncertainty at the bioliq® plant is the determination of the heat carrier mass flow rate. There is no direct measurement of this flow of hot abrasive solid particles in the process, so calculations are based on calibration data from dosing experiments without biomass. These experiments were performed under similar process conditions as during pyrolysis operation, but at more ideal boundary conditions. The uncertainty of the heat carrier mass flow rate is estimated with ca. 30 % relative uncertainty. Thus, the specific heat demands would vary from ca. 0.8 to 1.5 MJ kg^{-1} for both miscanthus campaigns and 0.6 to 1.1 MJ kg^{-1} for wheat straw campaigns 2015-2018.
Apart from the determination of heat carrier mass flow rate, temperature makes use of present state-of-the-art equipment applied in industry and not that of academia. Consequently, there is room for improving the precision of the temperature difference measurements across the pyrolysis reactor, too.

4.3 Comparison bioliq® and Python results

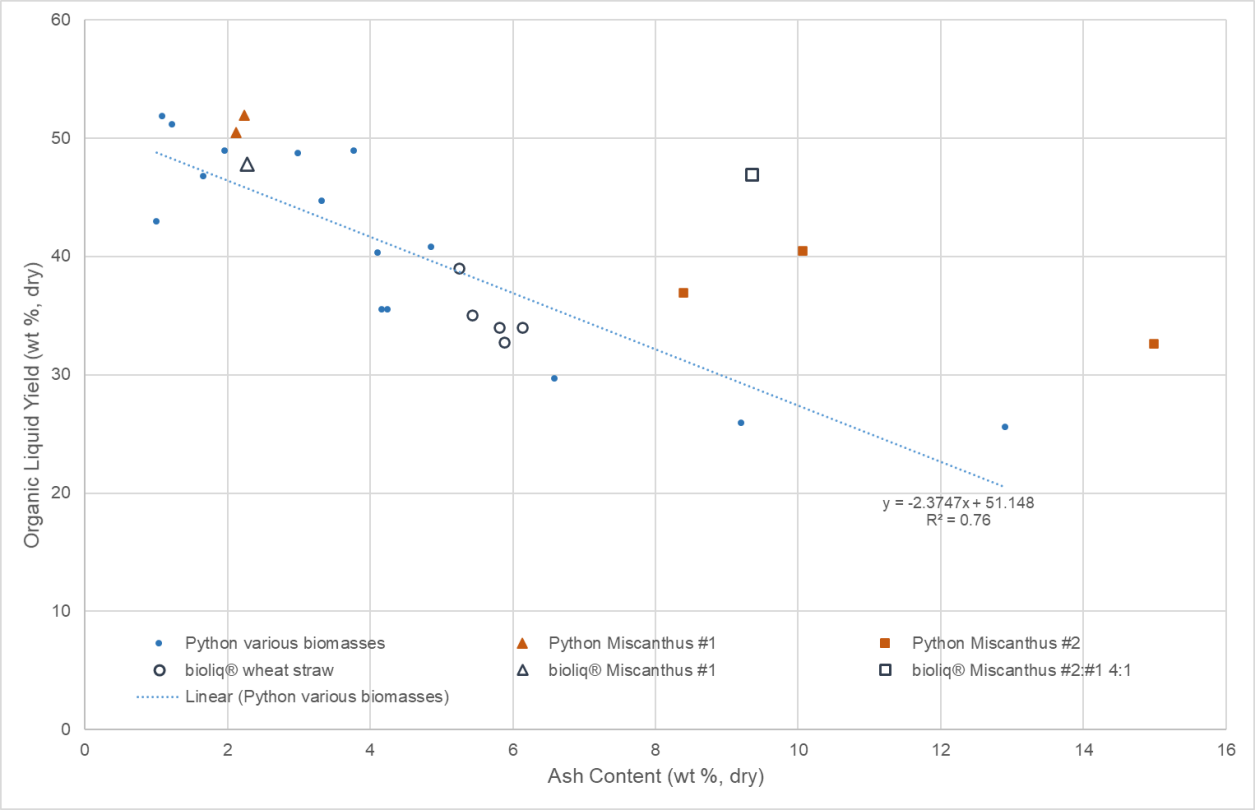

Figure 6 shows the organic liquid yield as a function of the ash content. The drawn simple linear regression refers to results of various types of biomass pyrolysed in the Python plant [19]. The higher the ash content, the lower becomes the OLY and the larger are the

fluctuations and deviations from the regression line. Reasons could be seen in the varying amount of those ash components that truly affect pyrolysis. Alkali metals, especially potassium, are known to catalyse consecutive pyrolysis reactions. This leads to a steep decrease in OLY with increasing alkali metal content of the feedstock during fast pyrolysis [35]. However, it has been more common to relate the total ash content of the feedstock to the OLY until now [19,36-38]; which obscures the actual catalytic effect since other major inorganic compounds, for example silicon, are largely inert. In the present case, the ash content is more than quadrupled from Miscanthus #1 to Miscanthus #2 governed by an increase in silicon while the potassium content 'only' doubled (see Table 5). This explains why the trend for the OLY deviates for the case of miscanthus from the more general trend observed in the Python plant. If the ash content of Miscanthus #1 was doubled (i.e. according to doubling the content of active inorganics such as potassium) its value would be at around 4-5 wt % and the trendline would predict 38-41 wt % OLY, which is well in line with the two Python miscanthus runs with quadrupled ash content, but only doubled potassium content. Based on these observations it is argued that the observed results are still in line with expectations and that the trend line based on overall ash content is misleading. The same argumentation could be applied to interprete the trend of bioliq® OLY as a function of ash content and the deviation of the Miscanthus #2 experimental campaign for the case of bioliq® (albeit with much less datapoints). Based on these observations it is recommended that future work should rather focus on active inorganics such as e.g. potassium instead of using the ash content.

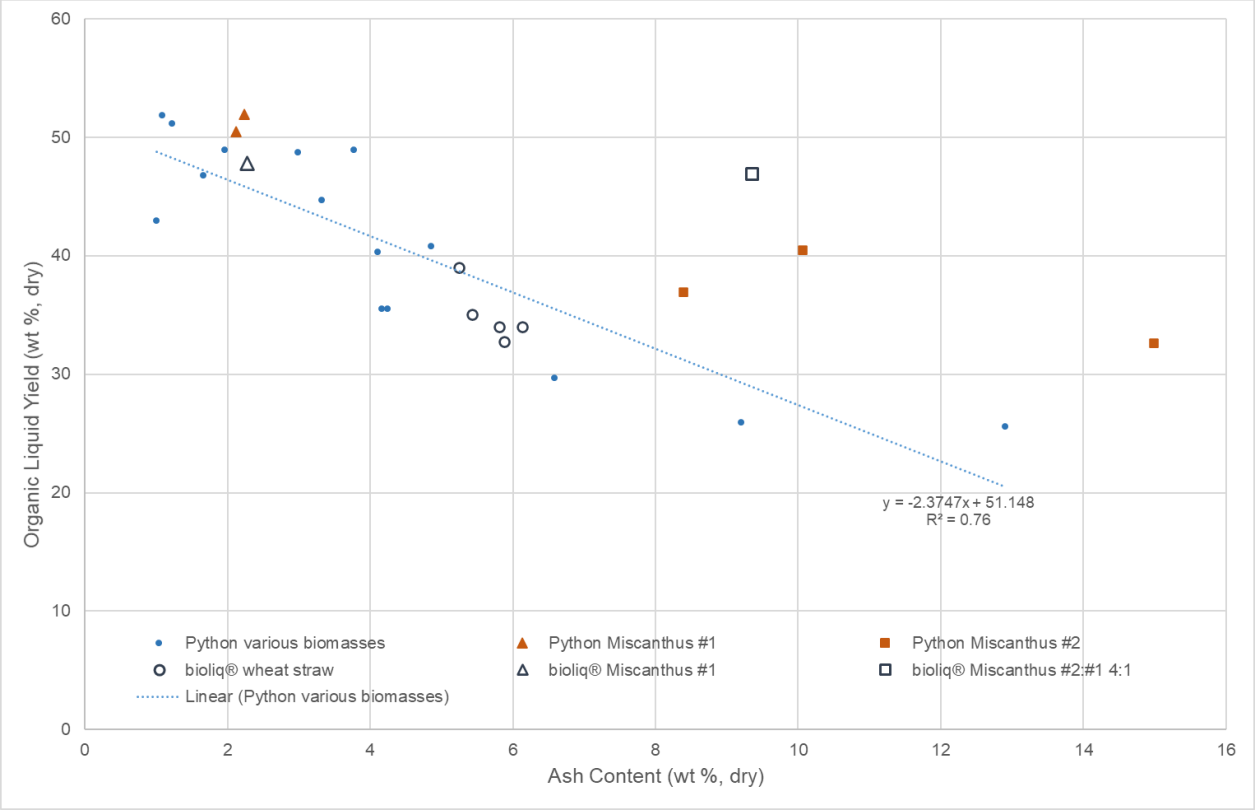

Figure 6: Organic liquid yield of pyrolysis products from bioliq® and Python as a function of biomass ash content

4.4 Product properties

The water content of the ORC is adjusted to stay between 12-15 wt % during the experimental campaign by varying condensation temperature in the first stage. Experience has shown that bio-oils with a water content of this range are homogeneous and easy to handle. The water content was measured by offline-analyses (samples of ORC periodically taken to the lab) every two hours, resulting in a significant lack in the control loop. This resulted in significant variations over the course of operation. Selected steady state data points (defined by a condensation temperature standard deviation <1 K over the course of 90 min) are presented in Figure 7. Surprisingly, there is no clear trend in the experimental data whereas it was shown to be very sensitive to temperature (lower condensation temperatures leading to higher water content) [26]. Vapour-liquid flash calculations have been conducted to better understand underlying effects and also account for different compositions arising from the varying feedstocks. The relative mean difference between model prediction and experimental data is 12%; the highest relative difference is 25 %. This is rated a reasonably good prediction of the observed water content. The tendency of the water content profile of the two ash rich feedstocks (i.e. wheat straw and Miscanthus #2) is well in line. Interestingly, the surrogate mixture representing the hot pyrolysis gas had substantially different water content in these two cases (32 and 27 %). It is concluded that the amount of water condensed in the first stage is not primarily depended on the total amount of water present but the results of a complex interaction of different components.

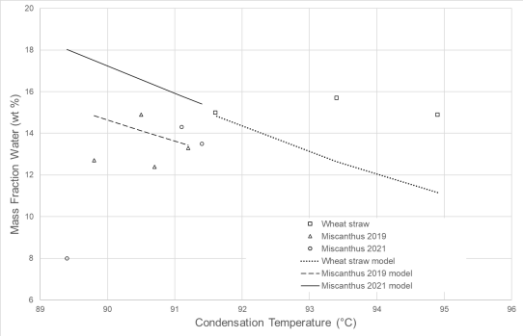

Figure 7: Water content in ORC as function of condensation temperature.

The solid content in ORC is lower in miscanthus experiments. It has been observed that the solid content increases over time until a certain steady state level is reached, which varies for different campaigns. The solid content in ORC from miscanthus was never as high as for ORC from wheat straw campaigns, which was 6-16 wt % [19]. Hence, the separation efficiency of the cyclone is higher for the particle size distribution of the char from miscanthus fast pyrolysis. Due to industry related working, the plant was not dismantled and cleaned (i.e.by sandblasting) after each campaign. Pipes were roughly mechanically cleaned with metal brushes. Permanent deposits on pipe walls may have affected the separation efficiency of the cyclone, letting expect a lower degree of separation. This was already observed in the earlier campaigns with wheat straw as feedstock. Before miscanthus was used as input material, the pipe section between reactor and cyclone and between cyclone and quench were dismantled and properly cleaned.

The carbon content in ORC is lower for miscanthus (straw: 53 - 55 wt %, miscanthus 48 - 50 wt %) as well as the calculated HHV based on the elemental composition using the correlation of Channiwala [39]. This is primarily an effect of the difference in solids content: if the carbon content of the solid fraction (char in ORC) is not attributed to the ORC, the carbon contents are of the same order of magnitude.

The chemical composition of the different ORC's are summarised in Figure 8. They are comparable to results published elsewhere for similar feedstocks [40]. Similar to other fast pyrolysis condensates recovered at around 60-90 °C, non-aromatic compounds have the

highest share of GC detectable species. Important contribution to this group are acetic acid (around 5 wt %), glycolaldehyde (2-3 wt %) and acetol (around 4 wt %). Other aldehydes and ketones have minor shares (<1 wt %), notably no aldehydes were observed in the ORC from wheat straw. There is a significant amount of propionic acid in the case of Miscanthus #2 that dominates the larger share of non-aromatic compounds observed in this case. Varying furans of minor concentration (<1 wt %) make up the heterocyclic compounds for all feedstocks. Aromatic compounds are similar for all feedstocks and show comparable amounts of phenols, guaiacols and syringols. Obviously, there is a significant difference in carbohydrates produced from miscanthus as compared to wheat straw. These are primarily made up of levoglucosan.

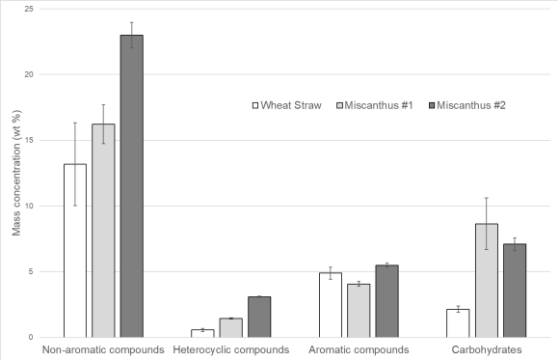

Figure 8: Composition of ORC based on different compound groups.

5 Conclusion

A change in feedstock for an existing pilot scale fast pyrolysis unit was tested successfully. This study was conducted in the bioliq® unit with a feedstock capacity of 500 kg h^{-1} and hardware features very close to an industrial operation. Consequently, important insights were gained for the flexibility of such an installations towards a change in feedstock and limitations that might arise from doing so. This unit was designed to pyrolyse wheat straw with relatively high ash content (around 6-7 wt %) which results in low organic liquid yield from fast pyrolysis conditions. The new feedstock tested was miscanthus, which is known to produce more organic liquids and thus poses a challenge to this existing installation. While it was possible to run this pilot unit on a continuous basis, feedstock capacity was reduced significantly compared to wheat straw. Observations during and after the campaign hint to the reactivity of the organic liquid products being of higher relevance than the actual amount of volatiles generated in the reactor. Plugging issues increase with the reactivity of liquids when hitting surfaces of process equipment.

The heat demand to sustain the pyrolysis process was estimated based on experimental process data to get data for large-scale infrastructures. Values found were from 0.8 to 1.5 MJ kg^{-1} for miscanthus and 0.6 to 1.1 MJ kg^{-1} for wheat straw. It was concluded that these values underestimate the true heat demand since laboratory scale results indicate higher heat demand for fast pyrolysis. This is most likely cause by uncertainties in quantifying the mass flow of heat carrier.

By comparing the product yield distribution with a smaller process development unit (10 kg h^{-1} feedstock capacity) it was shown that the organic liquid yield deviates from the trendline that represents a regression from a variety of feedstocks with different ash content. This is due to high deviations in the presence of alkali metals, which are known to strongly

affect pyrolysis reactions. Such differences are not reflected in the sum parameter of ash determination.

One of the main product characteristics for the use of FPBO is the water content, which has been controlled during the experimental campaign. Model prediction of phase equilibria at condensation temperature revealed good agreement with experimental data and showed a complex interaction of the total amount of water present in the pyrolysis gas entering the condenser and other organic compounds.

Acknowledgments

The Miscanthus experiments conducted in the process development unit Python were supported by the German Federal Ministry of Education and Research (BMBF) (grant number 031B0673A). Pilot plant operation and related R&D investigations are team work. The authors thank Daniel Richter and the bioliq®-team (operation and laboratory) for experimental support and extensive laboratory analyses.

References

[1] IEA (2022), *Bioenergy*, IEA, Paris https://www.iea.org/reports/bioenergy, License: CC BY 4.0
[2] I. Lewandowski, *Global Food Security-Agriculture Policy Economics and Environment*, 6, (2015) 34.
[3] B. Elbersen, Van Verzandvoort, M., Boogaard, S., Mucher, S., Cicarelli, T., Elbersen, W., Mantel, S., Bai, Z., MCallum, I., Iqbal, Y., Lewandowski, I., Von Cossel, M., Carrasco, J., Ramos, C.C., Sanz, M., Ciria, P., Monti, A., Consentino, S., Scordia, D., Eleftheriadis, I., in, WUR, Wageningen, Netherlands, 2018.
[4] M.S. Memon, J. Guo, A.A. Tagar, N. Perveen, C.Y. Ji, S.A. Memon and N. Memon, *Sustainability*, 10, (2018).
[5] V. Daioglou, E. Stehfest, B. Wicke, A. Faaij and D.P. van Vuuren, *Global Change Biology Bioenergy*, 8, (2016) 456.
[6] A. Brosowski, D. Thran, U. Mantau, B. Mahro, G. Erdmann, P. Adler, W. Stinner, G. Reinhold, T. Hering and C. Blanke, *Biomass & Bioenergy*, 95, (2016) 257.
[7] M.I. Cossel, Y.; Scordia, D.; Cosentino, S.L.; Elbersen, B.; Staritsky, I.; van Eupen, M.; Mantel, S.; Prysiazhniuk, O.; Mailiarenko, O.; Lewandowski, I., in, 2019.
[8] W. Gerwin, F. Repmann, S. Galatsidas, D. Vlachaki, N. Gounaris, W. Baumgarten, C. Volkmann, D. Keramitzis, F. Kiourtsis and D. Freese, *Soil*, 4, (2018) 267.
[9] I. Lewandowki, in Springer (Ed.), *Ecosystem Services and Carbon Sequestration in the Biosphere*, 2013, p. 333.
[10] M. Wagner, A. Mangold, J. Lask, E. Petig, A. Kiesel and I. Lewandowski, *Global Change Biology Bioenergy*, 11, (2019) 34.
[11] I. Lewandowski, J.C. Clifton-Brown, B. Andersson, G. Basch, D.G. Christian, U. Jorgensen, M.B. Jones, A.B. Riche, K.U. Schwarz, K. Tayebi and F. Teixeira, *Agronomy Journal*, 95, (2003) 1274.
[12] https://phyllis.nl/ , last access: 30.05.2023
[13] S.T. Wijeyekoon, K.; Corkran, H.; Bennett, P., in, IEA Bioenergy: Task 34, 2020.
[14] A.V. Bridgwater, *Biomass & Bioenergy*, 38, (2012) 68.
[15] J.A. Garcia-Nunez, M.R. Pelaez-Samaniego, M.E. Garcia-Perez, I. Fonts, J. Abrego, R.J.M. Westerhof and M. Garcia-Perez, *Energy & Fuels*, 31, (2017) 5751.
[16] G. Perkins, T. Bhaskar and M. Konarova, *Renewable & Sustainable Energy Reviews*, 90, (2018) 292.
[17] C.E. Greenhalf, D.J. Nowakowski, A.B. Harms, J.O. Titiloye and A.V. Bridgwater, *Fuel*, 108, (2013) 216.
[18] A. Oasmaa, Y. Solantausta, V. Arpiainen, E. Kuoppala and K. Sipila, *Energy & Fuels*, 24, (2010) 1380.
[19] A. Niebel, A. Funke, C. Pfitzer, N. Dahmen, N. Weih, D. Richter and B. Zimmerlin, *Energy & Fuels*, 35, (2021) 11333.
[20] A. Funke, D. Richter, A. Niebel, N. Dahmen and J. Sauer, *Jove-Journal of Visualized Experiments*, (2016).
[21] I. Lewandowski, J.M.O. Scurlock, E. Lindvall and M. Christou, *Biomass & Bioenergy*, 25, (2003) 335.
[22] https://ec.europa.eu/research-and-innovation/en/horizon-magazine/wheat-straw-waste-could-be-basis-greener-chemicals, last access: 30.05.2023
[23] https://materialarchiv.ch/de/ma:material_1391, last access 30.05.2023
[24] https://www.dbfz.de/fileadmin/user_upload/Referenzen/Broschueren/DBFZ_Strohmarkt_in_Deutschland.pdf, last access: 30.05.2023
[25] https://www.grace-bbi.eu/, last access 30.05.2023

[26] Y. Ille, F. Krohl, A. Velez, A. Funke, S. Pereda, K. Schaber and N. Dahmen, *Journal of Analytical and Applied Pyrolysis*, 135, (2018) 260.
[27] M. Windt, D. Meier, J.H. Marsman, H.J. Heeres and S. de Koning, *Journal of Analytical and Applied Pyrolysis*, 85, (2009) 38.
[28] https://www.tfz.bayern.de/mam/cms08/rohstoffpflanzen/dateien/bericht_18_geschuetzt.pdf, last access 30.05.2023
[29] M. Bergs, X.T. Do, J. Rumpf, P. Kusch, Y. Monakhova, C. Konow, G. Voelkering, R. Pude and M. Schulze, *Rsc Advances*, 10, (2020) 10740.
[30] A. Mangold, I. Lewandowski, J. Mohring, J. Clifton-Brown, J. Krzyzak, M. Mos, M. Pogrzeba and A. Kiesel, *Global Change Biology Bioenergy*, 11, (2019) 21.
[31] N. Dahmen, J. Abeln, M. Eberhard, T. Kolb, H. Leibold, J. Sauer, D. Stapf and B. Zimmerlin, *Wiley Interdisciplinary Reviews-Energy and Environment*, 6, (2017).
[32] E. Henrich, N. Dahmen, F. Weirich, R. Reimert and C. Kornmayer, *Fuel Processing Technology*, 143, (2016) 151.
[33] W.S.L. Mok and M.J. Antal, *Thermochimica Acta*, 68, (1983) 165.
[34] D.E. Daugaard and R.C. Brown, *Energy & Fuels*, 17, (2003) 934.
[35] E. Pienihakkinen, C. Lindfors, T. Ohra-aho and A. Oasmaa, *Energy & Fuels*, 36, (2022) 3654.
[36] A. Oasmaa, T. Sundqvist, E. Kuoppala, M. Garcia-Perez, Y. Solantausta, C. Lindfors and V. Paasikallio, *Energy & Fuels*, 29, (2015) 4373.
[37] A. Trubetskaya, M.T. Timko and K. Umeki, *Applied Energy*, 257, (2020).
[38] R. Fahmi, A. Bridgwater, I. Donnison, N. Yates and J.M. Jones, *Fuel*, 87, (2008) 1230.
[39] S.A. Channiwala and P.P. Parikh, *Fuel*, 81, (2002) 1051.
[40] S. Conrad, C. Blajin, T. Schulzke and G. Deerberg, *Environmental Progress & Sustainable Energy*, 38, (2019).

Figure

Click here to access/download;Figure;Figure 2_Mass balances miscanthus.xlsx

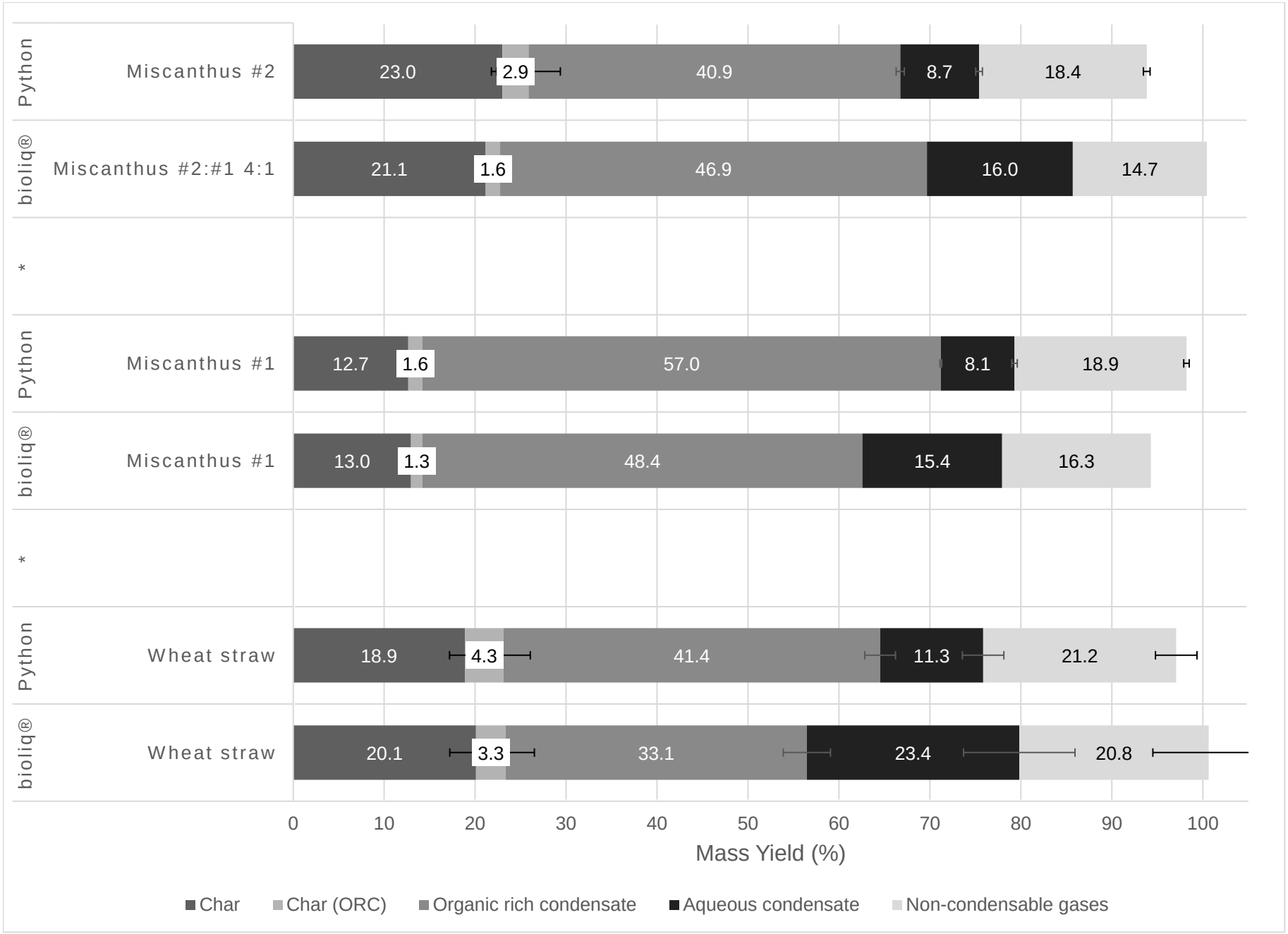

Mean values

		Char	Char (ORC)	Organic rich condensate
bioliq®	Wheat straw	20.1	3.3	33.1
Python *	Wheat straw	18.9	4.3	41.4
bioliq®	Miscanthus #1	13.0	1.3	48.4
Python *	Miscanthus #1	12.7	1.6	57.0
bioliq®	Miscanthus #2:#1 4:1	21.1	1.6	46.9
Python	Miscanthus #2	23.0	2.9	40.9

einzelne Versuche:

		Char	Organic rich condensate
bioliq	*Wheat straw*	*20.1*	*33.1*
Python	*Wheat straw*	*18.9*	*41.4*
bioliq	Miscanthus #1	13.0	48.4

Python	Miscanthus #1.1	#REF!	#REF!	
Python	Miscanthus #1.2	#REF!	#REF!	
bioliq	Miscanthus #2	21.1		46.9
Python	Miscanthus #2.1	#REF!	#REF!	
Python	Miscanthus #2.2	#REF!	#REF!	
Python	Miscanthus #2.3	#REF!	#REF!	

			STD Deviation
Aqueous condensate	Non-condensable gases	Sum	Char
23.4	20.8	100.6	2.9
11.3	21.2	97.1	1.7
15.4	16.3	94.3	
8.1	18.9	98.2	0.0
16.0	14.7	100.4	
8.7	18.4	93.8	1.2

Aqueous condensate	Non-condensable gases	Sum
23.4	*20.8*	*97.4*
11.3	*21.2*	*92.8*
15.4	16.3	93.0

#REF!	#REF!	#REF!
#REF!	#REF!	#REF!
16.0	14.7	98.8
#REF!	#REF!	#REF!
#REF!	#REF!	#REF!
#REF!	#REF!	#REF!

char (ORC)	Organic rich condensate	Aqueous condensate	Non-condensable gases
1.3	3.1	2.6	6.1
2.1	2.9	1.7	2.3
0.1	1.1	0.1	0.3
0.1	3.5	0.4	0.4

Figure

Click here to access/download;Figure;Figure 3_Comparison pressure dosing.xlsx

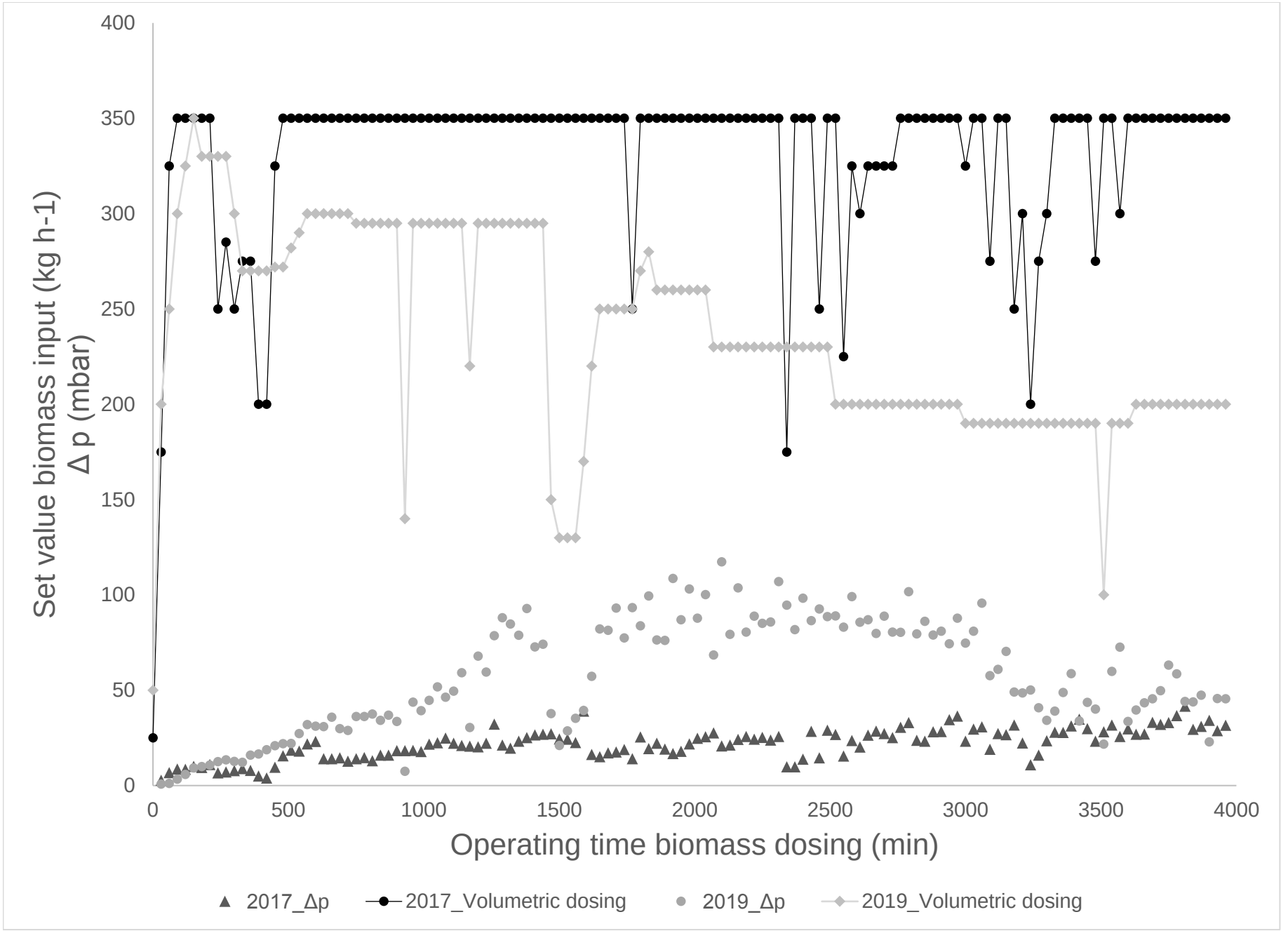

	2017		2019	
min operation	**CP 32418 XQ01**	**H 32106 KG_H XQ02**	**CP 32418**	**H 32106 KG_H XQ02**
0	-0.2	25.0	-1.6	50.0
30	2.8	175.0	0.8	200.0
60	6.8	325.0	1.1	250.0
90	8.7	350.0	3.4	300.0
120	8.6	350.0	5.8	325.0
150	10.1	350.0	9.3	350.0
180	9.5	350.0	9.9	330.0
210	11.1	350.0	10.8	330.0
240	6.7	250.0	12.6	330.0
270	7.2	285.0	13.5	330.0
300	7.9	250.0	12.7	300.0
330	8.9	275.0	12.2	270.0
360	8.0	275.0	16.0	270.0
390	5.0	200.0	16.6	270.0
420	4.0	200.0	18.8	270.0
450	9.6	325.0	21.0	272.0
480	15.6	350.0	22.0	272.0
510	18.6	350.0	22.1	282.0
540	18.1	350.0	27.3	290.0
570	21.9	350.0	32.0	300.0
600	23.1	350.0	31.2	300.0
630	14.1	350.0	31.0	300.0
660	14.1	350.0	35.9	300.0
690	14.5	350.0	29.8	300.0
720	12.8	350.0	28.9	300.0
750	14.1	350.0	36.2	295.0
780	14.7	350.0	36.2	295.0
810	13.0	350.0	37.6	295.0
840	16.0	350.0	34.2	295.0
870	16.0	350.0	36.9	295.0
900	18.3	350.0	33.6	295.0
930	18.3	350.0	7.5	140.0
960	18.5	350.0	43.7	295.0
990	17.9	350.0	39.3	295.0

min operation	CP 32418 XQ01	H 32106 KG_H XQ02	CP 32418	H 32106 KG_H XQ02
1020	21.7	350.0	44.7	295.0
1050	22.5	350.0	51.8	295.0
1080	25.0	350.0	46.4	295.0
1110	22.2	350.0	49.5	295.0
1140	21.0	350.0	59.2	295.0
1170	20.7	350.0	30.5	220.0
1200	20.4	350.0	68.0	295.0
1230	22.3	350.0	59.5	295.0
1260	32.3	350.0	78.6	295.0
1290	21.3	350.0	88.1	295.0
1320	19.6	350.0	84.7	295.0
1350	23.3	350.0	78.9	295.0
1380	25.1	350.0	92.9	295.0
1410	26.6	350.0	72.7	295.0
1440	27.0	350.0	74.1	295.0
1470	27.2	350.0	37.7	150.0
1500	24.4	350.0	21.0	130.0
1530	24.4	350.0	28.7	130.0
1560	22.5	350.0	35.3	130.0
1590	39.0	350.0	39.4	170.0
1620	16.3	350.0	57.3	220.0
1650	15.1	350.0	82.2	250.0
1680	17.1	350.0	81.5	250.0
1710	17.6	350.0	93.1	250.0
1740	18.9	350.0	77.4	250.0
1770	14.1	250.0	93.4	250.0
1800	25.6	350.0	83.8	270.0
1830	19.4	350.0	99.4	280.0
1860	22.2	350.0	76.3	260.0
1890	19.1	350.0	76.2	260.0
1920	16.8	350.0	108.7	260.0
1950	18.0	350.0	86.9	260.0
1980	21.8	350.0	103.1	260.0
2010	24.8	350.0	87.9	260.0
2040	25.6	350.0	100.2	260.0

min operation	CP 32418 XQ01	H 32106 KG_H XQ02	CP 32418	H 32106 KG_H XQ02
2070	27.6	350.0	68.5	230.0
2100	20.8	350.0	117.4	230.0
2130	21.2	350.0	79.3	230.0
2160	24.2	350.0	103.7	230.0
2190	25.8	350.0	80.5	230.0
2220	24.3	350.0	88.9	230.0
2250	25.2	350.0	85.1	230.0
2280	23.9	350.0	85.8	230.0
2310	25.8	350.0	107.0	230.0
2340	9.9	175.0	94.6	230.0
2370	9.9	350.0	81.8	230.0
2400	13.9	350.0	98.3	230.0
2430	28.5	350.0	86.5	230.0
2460	14.6	250.0	92.6	230.0
2490	29.1	350.0	88.6	230.0
2520	26.8	350.0	89.0	200.0
2550	15.5	225.0	83.1	200.0
2580	23.6	325.0	99.2	200.0
2610	20.2	300.0	85.6	200.0
2640	26.5	325.0	87.0	200.0
2670	28.6	325.0	79.9	200.0
2700	27.3	325.0	88.9	200.0
2730	25.1	325.0	80.6	200.0
2760	30.6	350.0	80.4	200.0
2790	33.0	350.0	101.7	200.0
2820	23.7	350.0	79.6	200.0
2850	23.3	350.0	86.2	200.0
2880	28.3	350.0	79.0	200.0
2910	28.3	350.0	80.9	200.0
2940	34.6	350.0	74.4	200.0
2970	36.5	350.0	87.8	200.0
3000	23.3	325.0	74.7	190.0
3030	29.6	350.0	81.0	190.0
3060	30.8	350.0	95.7	190.0
3090	19.0	275.0	57.7	190.0

min operation	CP 32418 XQ01	H 32106 KG_H XQ02
3120	27.3	350.0
3150	26.7	350.0
3180	31.8	250.0
3210	22.3	300.0
3240	10.9	200.0
3270	16.0	275.0
3300	23.5	300.0
3330	28.0	350.0
3360	27.9	350.0
3390	31.2	350.0
3420	34.8	350.0
3450	29.8	350.0
3480	23.3	275.0
3510	28.2	350.0
3540	31.8	350.0
3570	25.8	300.0
3600	29.7	350.0
3630	26.9	350.0
3660	27.0	350.0
3690	33.1	350.0
3720	32.1	350.0
3750	33.1	350.0
3780	36.7	350.0
3810	41.6	350.0
3840	29.5	350.0
3870	31.1	350.0
3900	34.3	350.0
3930	28.8	350.0
3960	31.6	350.0

2017_Δp

CP 32418	H 32106 KG_H XQ02
60.9	190.0
70.4	190.0
49.0	190.0
48.6	190.0
50.1	190.0
40.8	190.0
34.2	190.0
39.1	190.0
48.8	190.0
58.7	190.0
33.9	190.0
43.7	190.0
40.1	190.0
21.7	100.0
59.9	190.0
72.6	190.0
33.6	190.0
39.7	200.0
43.4	200.0
45.6	200.0
49.8	200.0
63.2	200.0
58.7	200.0
44.2	200.0
43.9	200.0
47.4	200.0
23.0	200.0
45.7	200.0
45.5	200.0

2019_Δp

Figure

Click here to access/download;Figure;Figure 4_Volume flow rate.xlsx

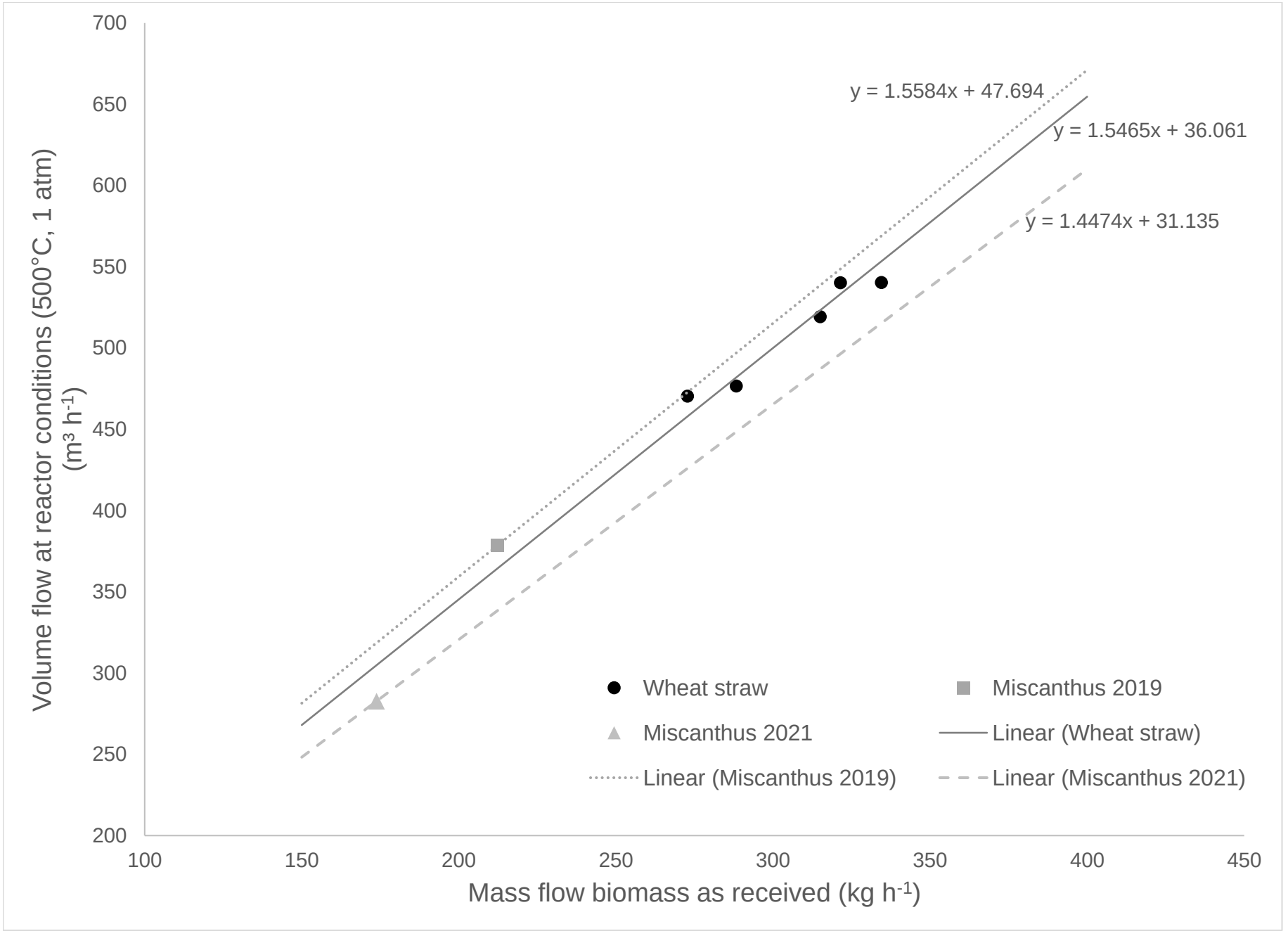

			Weizenstroh
	bioliq		**2015-05/06**
Massenstrom Biomasse	kg h-1		272.8
	Dosierung		**Volumenstrom**
werte bei konstantem N2-Fluss		**150**	**274**
		200	**354**
		250	**434**
		300	**514**
		350	**594**
		400	**674**
Volumenstrom gesamt 1 (@ 500 °C, 1 bar)	**m3 h-1**		**470**

			Miscanthus		
2015-46/47	**2016-29**	**2017-19/20**	**2018**	**2019**	**2021**
334.5	288.3	315	321.5	212.3	173.8
n in m³/h					
261	**263**	**268**	**275**	**281**	**248**
337	**340**	**344**	**352**	**359**	**321**
412	**417**	**420**	**429**	**437**	**393**
488	**495**	**496**	**507**	**515**	**465**
564	**572**	**573**	**584**	**593**	**538**
639	**649**	**649**	**662**	**671**	**610**
540	**477**	**519**	**540**	**379**	**283**

Mittelwert Stroh	stabw
stroh mittel	
268	**6**
345	**7**
423	**9**
500	**10**
577	**12**
655	**13**
Stroh mittel	

Figure

Click here to access/download;Figure;Figure 5_Heat demand reactor.xlsx

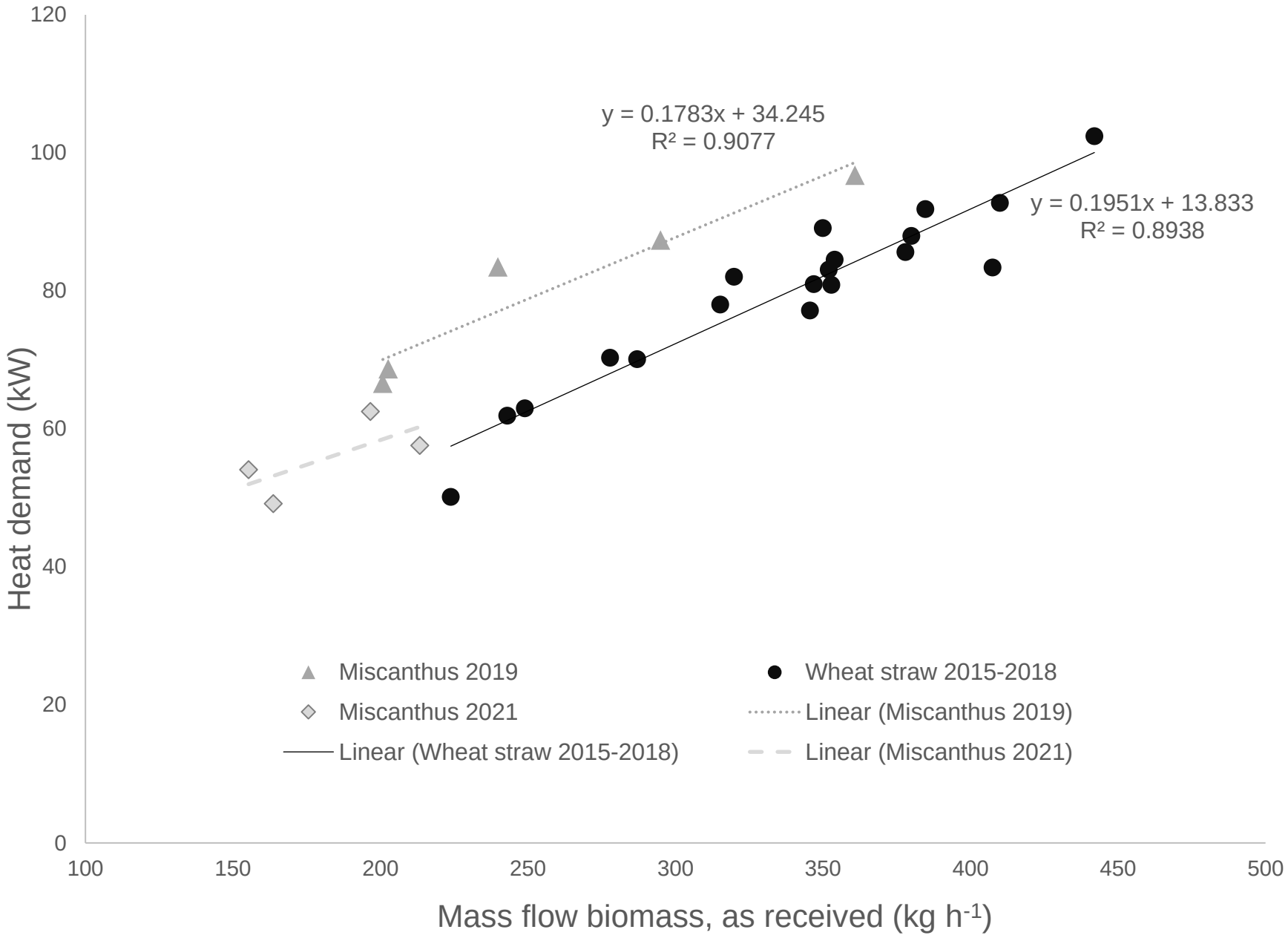

	kg/h	kW	kJ/kg
Miscanthus-2019-BZ1 - 295 kg	**294.9**	87	1066
Miscanthus-2019-BZ2 - 240 kg	**239.8**	83	1253
Miscanthus-2019-BZ3 - 203 kg	**202.6**	69	1221
Miscanthus-2019-BZ4 - 201 kg	**200.8**	67	1194
Mis 2019 - 11.10. 19:10-21:10 Uhr	**360.9**	97	965
Miscanthus-2021-BZ1 - 213 kg	**213.3**	58	972
Miscanthus-2021-BZ2 - 197 kg	**196.6**	63	1145
Miscanthus-2021-BZ3 - 164 kg	**163.7**	49	1081
Miscanthus-2021-BZ4 - 155 kg	**155.3**	54	1254
WZ 2018-10-09 22:10-23:10 Uhr	**223.9**	50	806
WZ 2018-10-10 02:55-03:45 Uhr	**277.9**	70	911
WZ 2017-05-17 21:30-22:30 Uhr	**243.0**	62	917
WZ 2015-11-13 19:20-19:50 Uhr	**287.0**	70	879
WZ 2015-11-14 14:20-15:20 Uhr	**249.0**	63	911
WZ 2015-01-29 17:10-21:10 Uhr	**315.2**	78	891
WZ 2015-01-30 04:00-07:00 Uhr	**319.9**	82	923
Wheat straw-2018-BZ1 - 354 kg	**354.0**	85	860
Wheat straw-2018-BZ2 - 347 kg	**346.9**	81	840
Wheat straw-2017-BZ1 - 346 kg	**345.6**	77	804
Wheat straw-2017-BZ2 - 353 kg	**352.9**	81	825
Wheat straw-2017-BZ3 - 408 kg	**407.5**	83	737
Wheat straw-2016-BZ1 - 410 kg	**410.0**	93	814
Wheat straw-2016-BZ2 - 380 kg	**380.0**	88	833
Wheat straw-2015-KW46+47-BZ1 - 442 kg	**442.0**	102	834
Wheat straw-2015-KW46+47-BZ2 - 352 kg	**352.0**	83	849
Wheat straw-2015-KW46+47-BZ3 - 378 kg	**378.0**	86	815
Wheat straw-2015-KW5+6-BZ1 - 385 kg	**384.7**	92	859
Wheat straw-2015-KW5+6-BZ2 - 350 kg	**350.0**	89	916

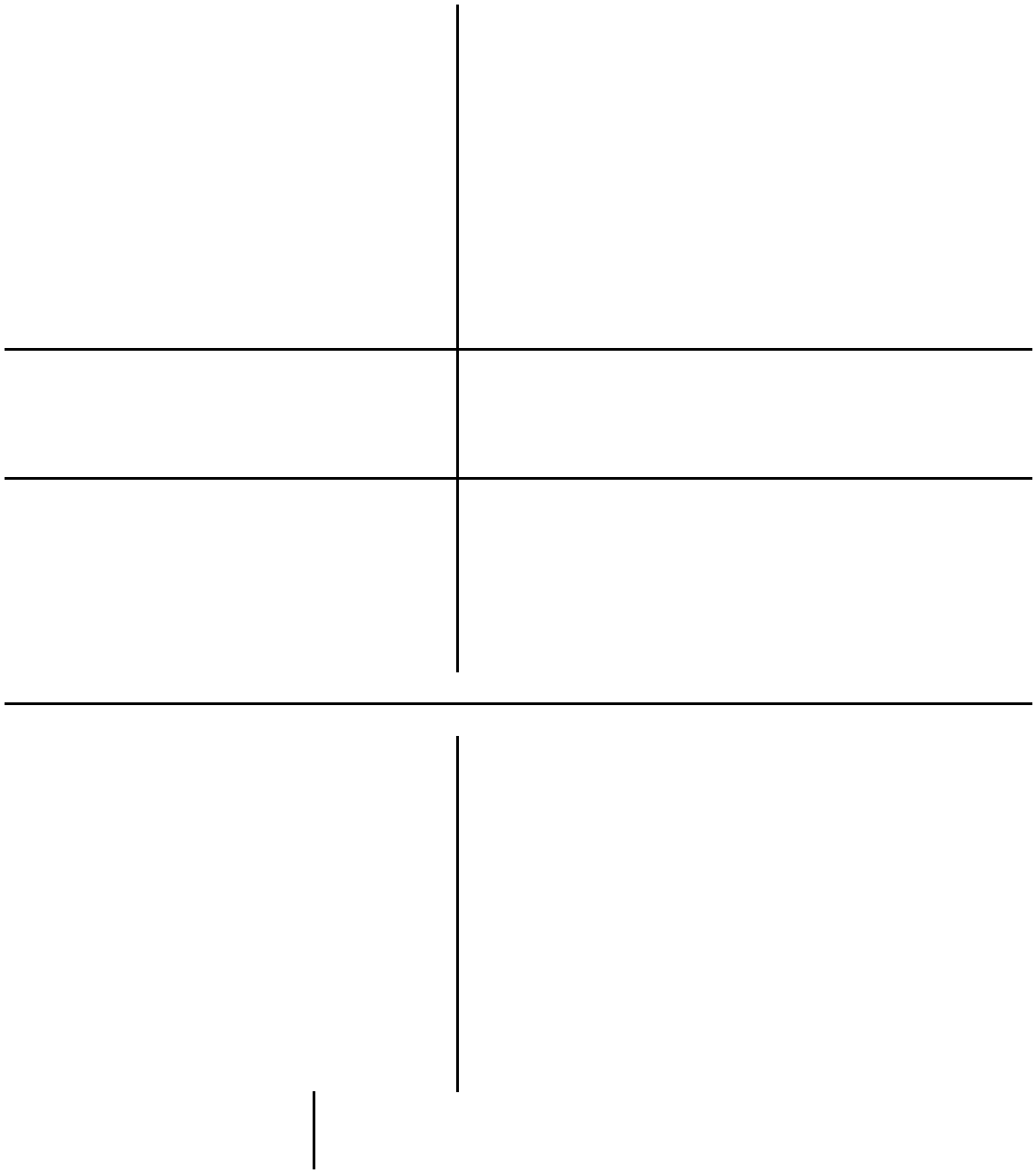

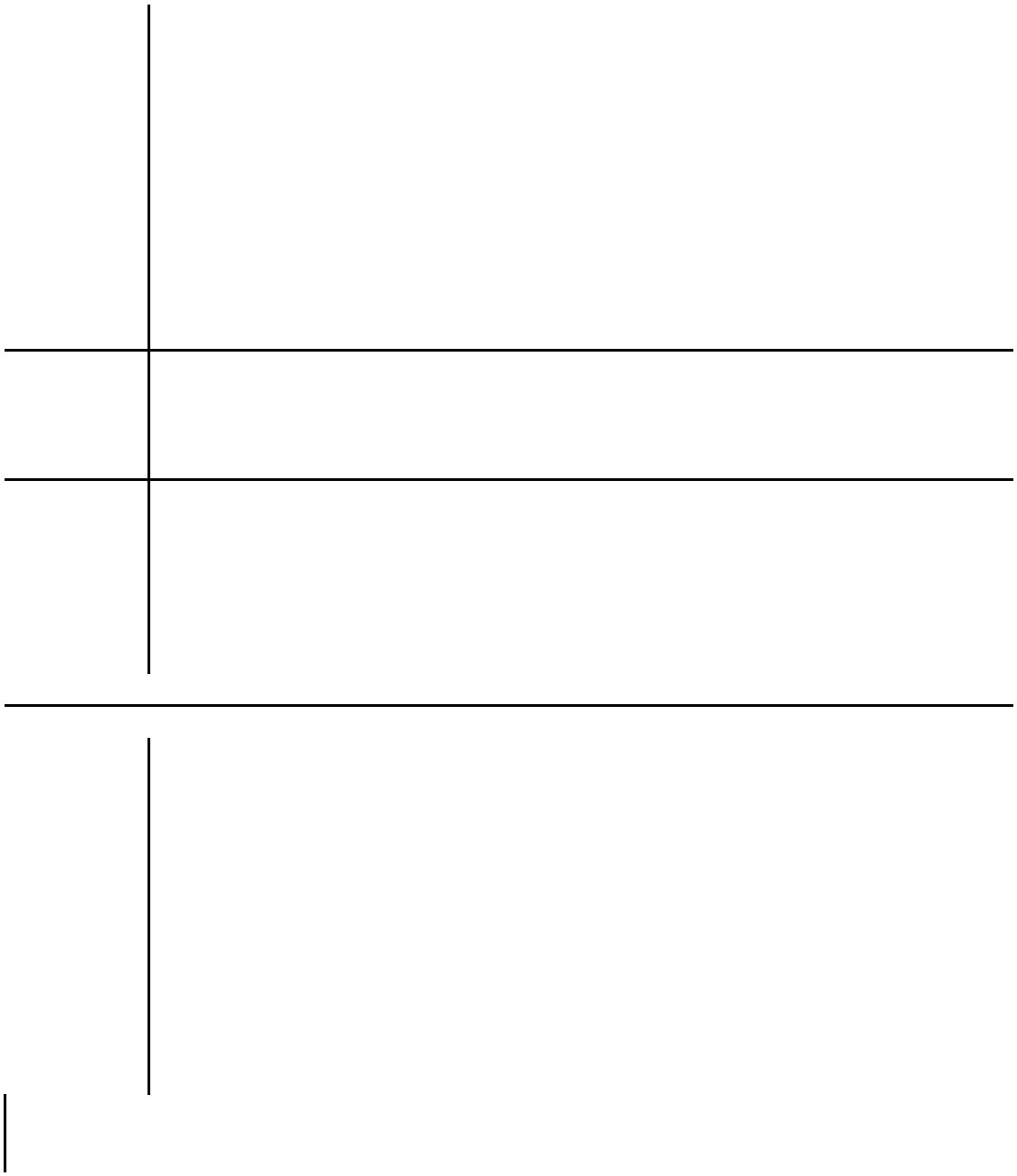

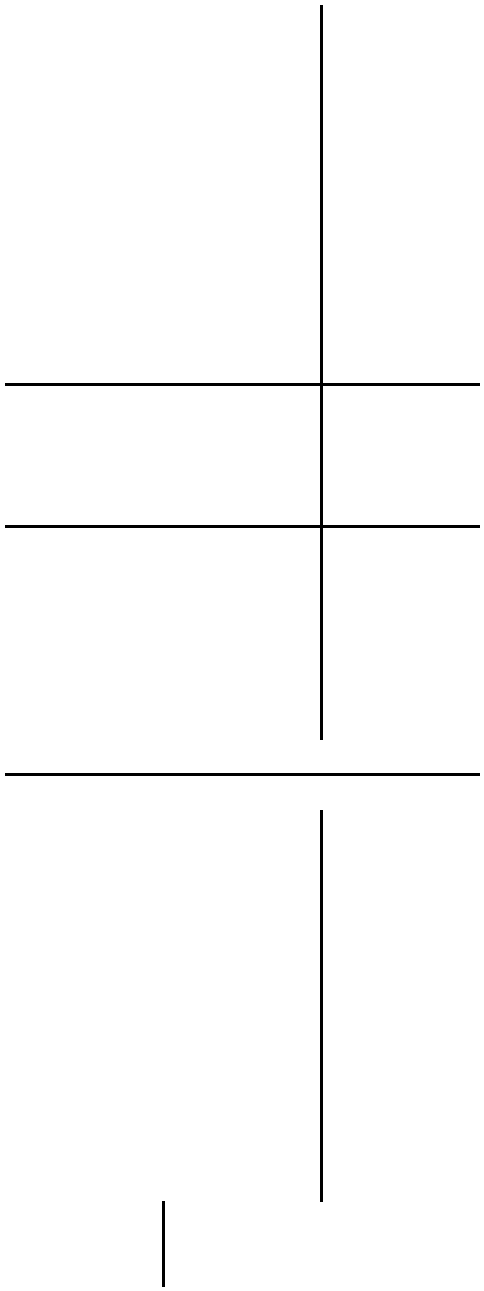

Figure

Click here to access/download;Figure;Figure 6_Organic liquid yield_ash.xlsx

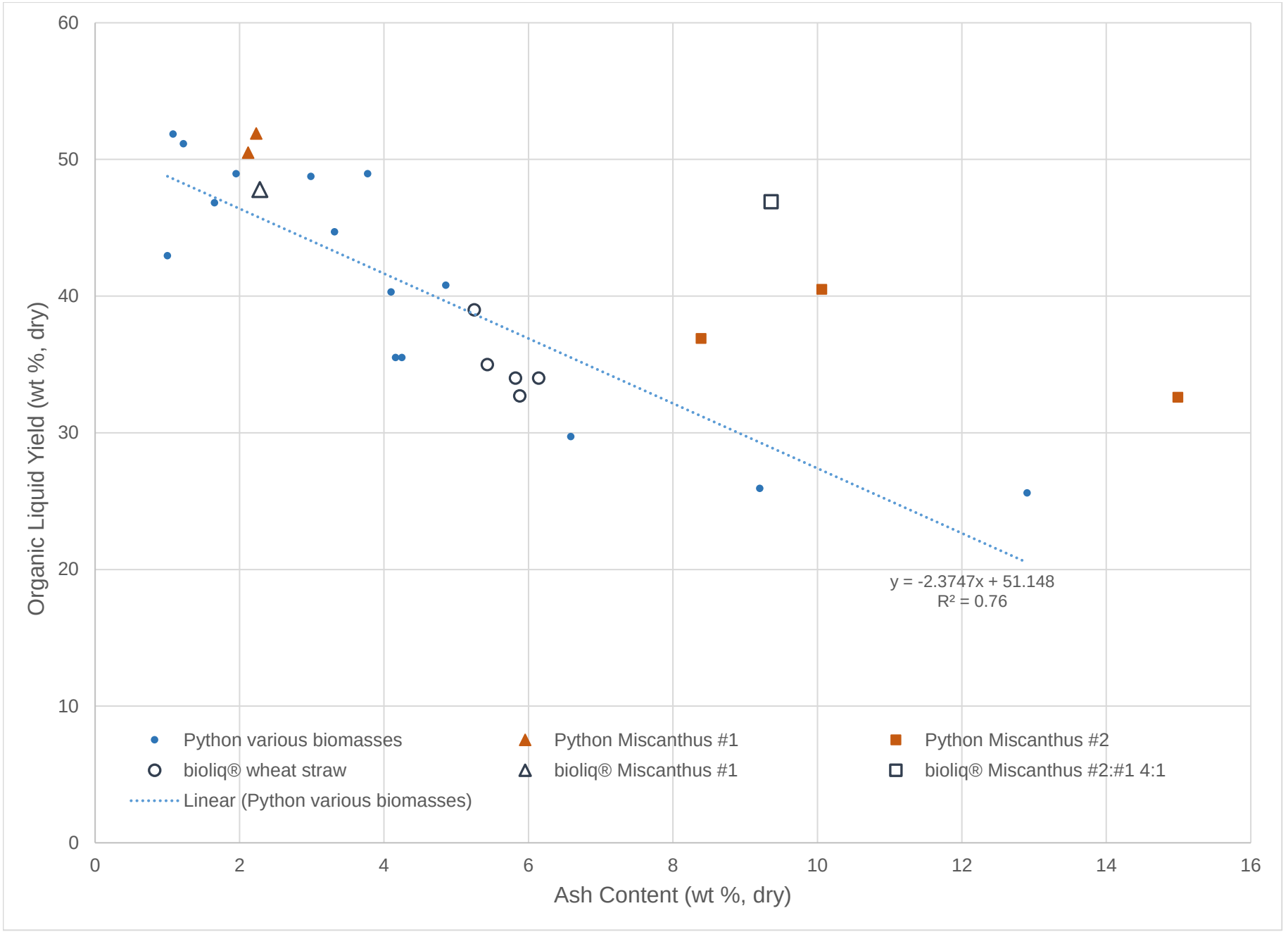

Python

Biomass	Ash Content (%), dry	OrgLiqYield (%), dry
Wheat Straw #1	9.2	25.9
Wheat Straw #2	12.9	25.6
Wheat Straw #3	6.6	29.7
Beech Wood #1	1.2	51.2
Beech Wood #2	1.1	51.9
Scrap Wood	1.7	46.8
Forest Residue Mix	4.2	35.5
Poplar Wood	2.0	49.0
Oil Palm Kernel Shells #1	4.1	40.3
Oil Palm Kernel Shells #2	3.3	44.7
Coconut Shells	1.0	43.0
Bagasse/Sugar Cane Straw	3.8	49.0
Sugar Cane Straw	4.9	40.8
Sugar Cane Bagasse	3.0	48.8
Coffee	4.2	35.5
Miscanthus 2019 #1	2.12	50.5
Miscanthus 2019 #2	2.23	51.9
Miscanthus 2021 #1	14.99	32.6
Miscanthus 2021 #2	8.39	36.9
Miscanthus 2021 #3	10.06	40.5

bioliq

	Campaign	Ash Content (%), dry
27.1		
	2015 KW 5+6	5.25
	2015 KW 46+47	6.14
	2016 KW 29+30	5.43
	2017 KW 19+20	5.88
	2018 KW 41-43	5.82
	2019 Miscanthus	2.28
	2021 Miscanthus	9.36

OrgLiqYield (%), dry	
39	
34	
35	
32.7	
34	
47.8	
46.9	
	bioliq® Miscanthus #1
	bioliq® Miscanthus #2:#1 4:1
	bioliq® wheat straw

Figure

Click here to access/download;Figure;Figure 7_Water content ORC.xlsx

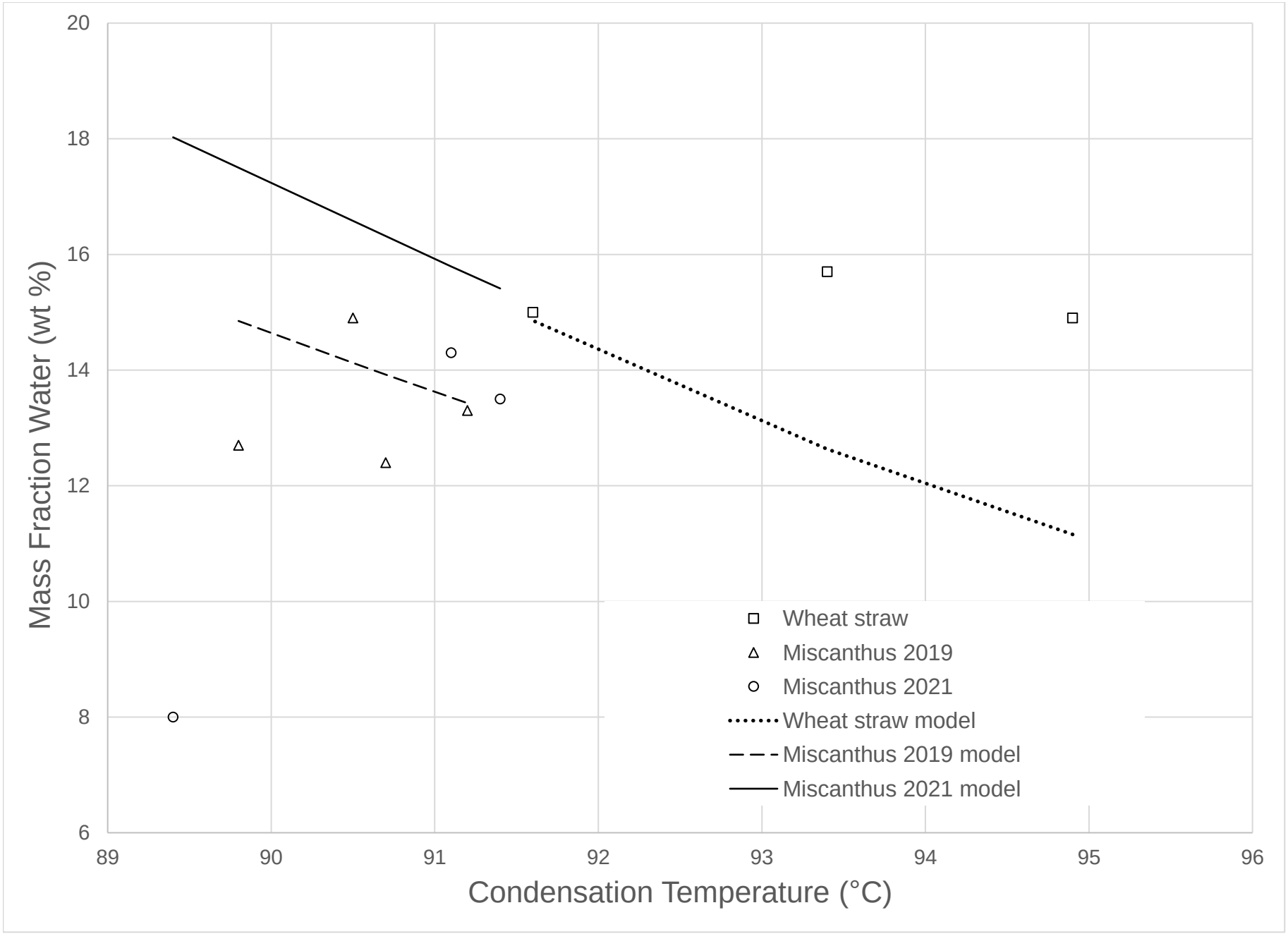

		Mean Conensation Temperature CT32404	Water (wt.%)	
WS	10/11/2018 3:30		94.9	14.9
Wheat straw	10/14/2018 2:30		93.4	15.7
	10/16/2018 2:30		91.6	15
not used:	10/15/2018 14:15		91.0	12.4
MS #1	10/14/2019 2:30		89.8	12.7
Miscanthus 2(	10/12/2019 16:30		90.5	14.9
	10/13/2019 10:30		90.7	12.4
	10/13/2019 2:30		91.2	13.3
not used:	10/12/2019 10:30		92.8	17
MS #2	7/4/2021 10:30		89.4	8
Miscanthus 2(	7/2/2021 10:30		91.1	14.3
	7/3/2021 10:30		91.4	13.5
not used:	7/1/2021 10:30		88.2	20.6

water (model)	abs percent dev	
11.2	25	WS model
12.6	20	Wheat straw model
14.9	1	
15.7	21	
14.8	17	MS #1 model
14.1	5	Miscanthus 2019 model
13.9	12	
13.4	1	
12.0	42	
18.0	125	MS #2 model
15.8	10	Miscanthus 2021 model
15.4	14	
19.6	5	

Figure

Click here to access/download;Figure;Figure 8_Composition ORC.xlsx

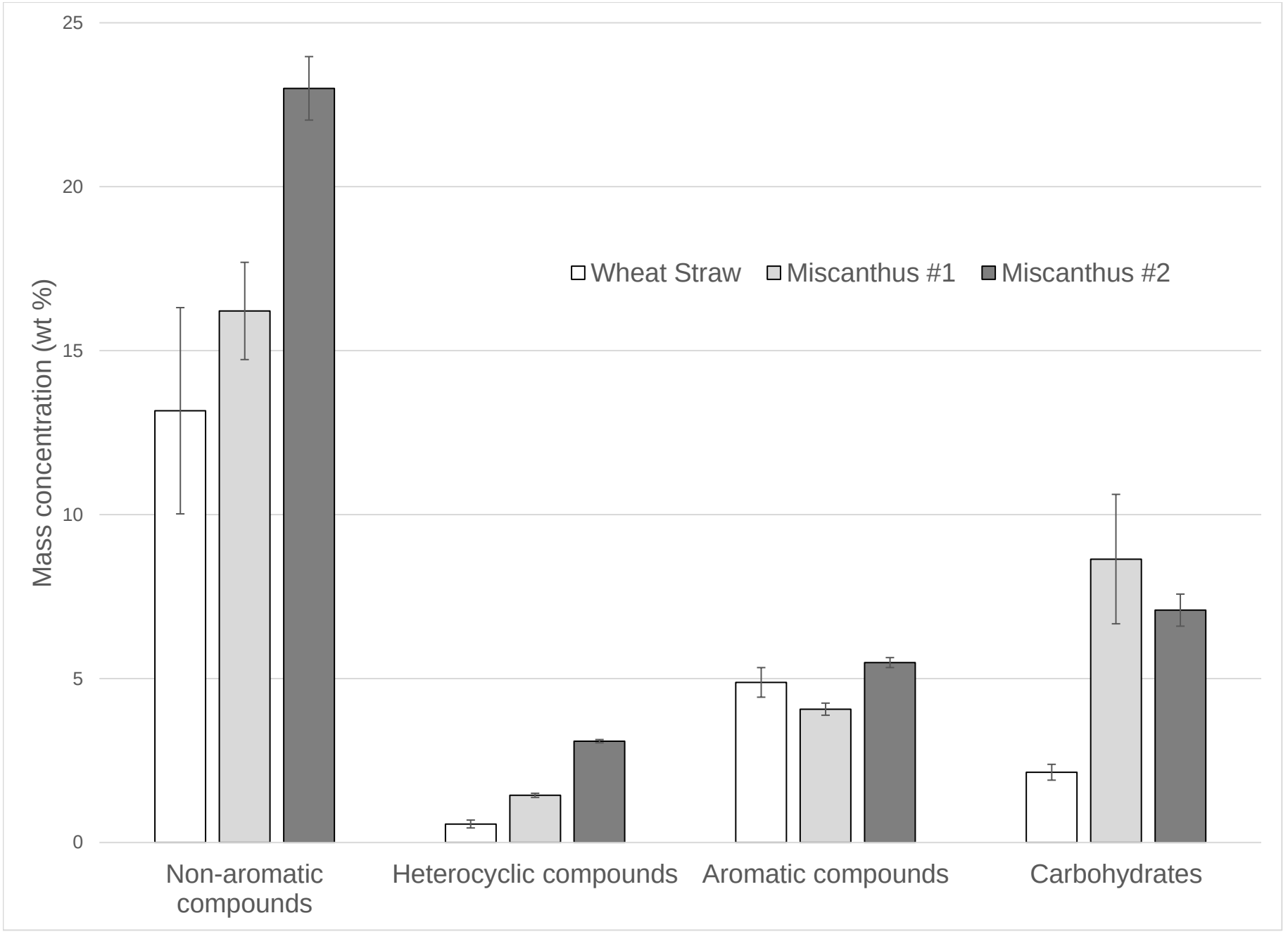

	Wheat Straw	ORC	Miscanthus #1	ORC
Non-aromatic compounds	13.17	3.15	16.21	1.48
Heterocyclic compounds	0.56	0.12	1.44	0.06
Aromatic compounds	4.88	0.45	4.07	0.18
Carbohydrates	2.14	0.24	8.64	1.97

Miscanthus #2	ORC
23.00	0.97
3.09	0.05
5.49	0.15
7.09	0.49

Figure

Click here to access/download;Figure;Figure1_Flow chart bioliq.jpg

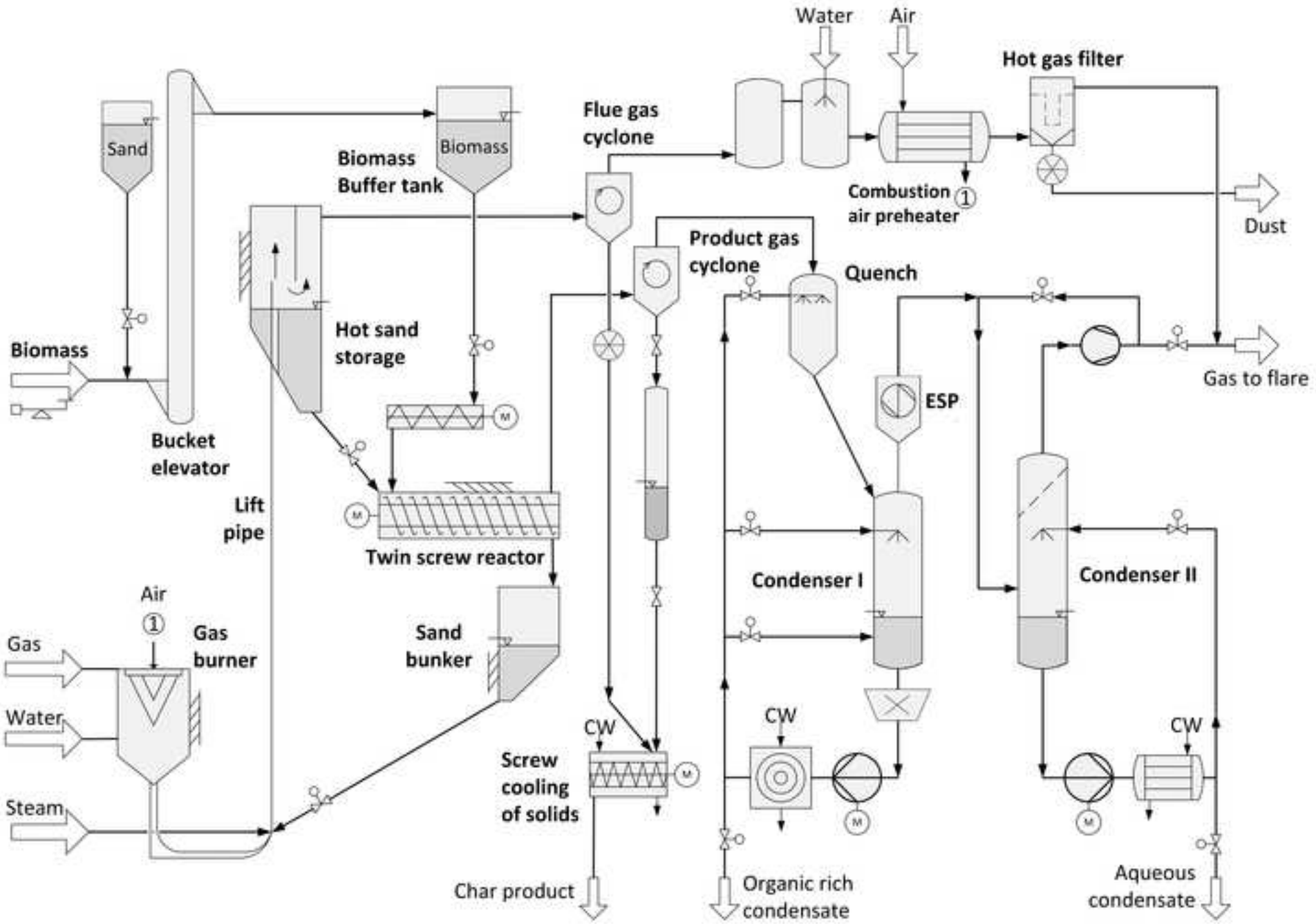

Declaration of interests

☒The authors declare that they have no known competing financial interests or personal relationships that could have appeared to influence the work reported in this paper.

☐The authors declare the following financial interests/personal relationships which may be considered as potential competing interests: